DATA ARTIKEL

Judul Artikel	: Numerical simulation for deformation characteristic of tea shoot under negative pressure guidance by the immersed boundary–lattice Boltzmann method
Nama Jurnal	: Biosystems Engineering
Nomor ISSN	: 15375110, 15375129
Vol, No, Bln Thn	: Vol.65, November, 2022
Penerbit	: Elsevier
DOI Artikel	: https://doi.org/10.1016/j.jocs.2022.101882
Terindeks	: Scopus, Q1
H-Index	: 117
SJR	: 1.02 (2021)

REKAP BUKTI KORESPONDENSI

Tanggal	Keterangan
06 Mei 2022	Review Invitation
10 Mei 2022	Agreeing Review
16 Mei 2022	Review Submission + Thank-you Note

(38) WhatsApp | Bismillah.pdf | Invitation to review for Bi | Editorial Manager® | Hindawi

mail.google.com/mail/u/0/?tab=rm#inbox/FMfcgzGpFqPWdzqgrDxmzttftdkDwXNx

Gmail YouTube Maps WhatsApp Kuliah Online Unive... New Tab

Gmail

Search mail

Compose

Inbox 154

Starred

Snoozed

Meet

New meeting

Join a meeting

Hangouts

Eflita

No recent chats
Start a new one

11 of 1,943

Invitation to review for Biosystems Engineering

Inbox

Fernando Auat Cheein <em@editorialmanager.com>

to me

Fri, May 6, 9:28 PM (4 days ago)

Manuscript Number: YBENG-D-22-00513
Numerical simulation for deformation characteristic of tea shoot under negative pressure guidance by the immersed boundary–lattice Boltzmann method
Yingpeng Zhu; Yikun Wei; Zhengdao Wang; Rongyang Wang; Chuanyu Wu; Jianneng Chen; Junhua Tong

Dear Dr. Yohana,

I would like to invite you to review the above referenced manuscript submitted by Dr Junhua Tong, as I believe it falls within your expertise and interest. The abstract for this manuscript is included below.

You should treat this invitation, the manuscript and your review as confidential. You must not share your review or information about the review process with anyone without the agreement of the editors and authors involved, even after publication. This also applies to other reviewers' "comments to author" which are shared with you on decision (and vice versa).

Please respond to this invitation at your earliest opportunity.

Review 3052022.docx | Bismillah.pdf | Show all

29°C Hujan ringan 14.00 10/05/2022

If you would like to review this paper, please click this link:
https://www.editorialmanager.com/ybeng/l.asp?i=191449&l=WCSN6HLM

If you have a conflict of interest or do not wish to review this paper, please click this link:
https://www.editorialmanager.com/ybeng/l.asp?i=191450&l=CLCXK35T

If you decline to review, I would appreciate your suggestions for alternate reviewers.

If, for any reason, the above links do not work, please log in as a reviewer at https://www.editorialmanager.com/ybeng/.

Since timely reviews are of utmost importance to authors, I would appreciate receiving your review within 21 days of accepting this invitation.

I hope you will be able to review this manuscript.

Thank you in advance for your contribution and time.

As a reviewer you are entitled to complimentary access to references, abstracts, and full-text articles on ScienceDirect and Scopus for 30 days. Full details on how to claim your access via Reviewer Hub (reviewerhub.elsevier.com) will be provided upon your acceptance of this invitation to review.

Please visit the Elsevier Reviewer Hub (reviewerhub.elsevier.com) to manage all your refereeing activities for this and other Elsevier journals on Editorial

(39) WhatsApp | Bismillah.pdf | Invitation to review for Bi | Editorial Manager® | Hindawi

mail.google.com/mail/u/0/?tab=rm#inbox/FMfcgzGpFqPWdzqgrDxmzttftdkDwXNx

Gmail YouTube Maps WhatsApp Kuliah Online Unive... New Tab

Gmail

Search mail

Compose

Inbox 154

Starred

Snoozed

Meet

New meeting

Join a meeting

Hangouts

Eflita

No recent chats
Start a new one

11 of 1,943

Thank you in advance for your contribution and time.

As a reviewer you are entitled to complimentary access to references, abstracts, and full-text articles on ScienceDirect and Scopus for 30 days. Full details on how to claim your access via Reviewer Hub (reviewerhub.elsevier.com) will be provided upon your acceptance of this invitation to review.

Please visit the Elsevier Reviewer Hub (reviewerhub.elsevier.com) to manage all your refereeing activities for this and other Elsevier journals on Editorial Manager.

Kind regards,

Fernando Auat Cheein
Associate Editor
Biosystems Engineering

Abstract:
At present, due to the shortage of tea picking labour force, realizing the mechanized picking of famous tea is urgent. Using negative pressure guidance is a feasible method, which can compensate the localization error of machine vision. In this paper, tea shoot with one bud and two leaves is taken as the study object, and a 'Y-type' tea physical model is established according to its physical properties. Moreover, the deformation characteristic of tea shoot under negative pressure guidance is studied by using the immersed boundary–lattice Boltzmann method. The purpose is to analyse the effects of pressure P, vertical deviation H and horizontal deviation W on the deformation characteristics of tea shoot quantitatively. The effectiveness of the numerical calculation method is

Review 3052022.docx | Bismillah.pdf | Show all

29°C Hujan ringan 14.01 10/05/2022

(39) WhatsApp | Bismillah.pdf | Invitation to review for Bi | Editorial Manager® | Hindawi

mail.google.com/mail/u/0/?tab=rm#inbox/FMfcgzGpFqPWdzqgrDxmzttftdkDwXNx

Gmail YouTube Maps WhatsApp Kuliah Online Unive... New Tab

Gmail

Search mail

11 of 1,943

Compose

Inbox 154

Starred

Snoozed

Meet

New meeting

Join a meeting

Hangouts

Eflita

No recent chats

Start a new one

verified by simulation tests. Results show that P determines fluid velocity, and the difference of steady leaf span (d s) is small when P is less than 0.990. In addition, setting P =

0.990, when H = 0 and W = 8, d s achieves a minimum value of 1.78. According to the above findings, this paper provides useful data and insights into the picking technology of famous tea based on negative pressure guidance.

*****

Please also note that authors have been invited to convert methods-related supplementary material into a MethodsX article (a detailed description of their methods). You may notice this change alongside the revised manuscript. You do not need to review this but may need to look at the files in order to confirm that any supporting information you requested is present there.

More information and support

FAQ: How do I respond to an invitation to review in Editorial Manager?

https://service.elsevier.com/app/answers/detail/a_id/28524/supporthub/publishing/

You will find guidance and support on reviewing, as well as information including details of how Elsevier recognizes reviewers, on Elsevier's Reviewer Hub:

https://www.elsevier.com/reviewers

FAQ: How can I reset a forgotten password?

https://service.elsevier.com/app/answers/detail/a_id/28452/supporthub/publishing/

For further assistance, please visit our customer service site: https://service.elsevier.com/app/home/supporthub/publishing/

Here you can search for solutions on a range of topics, find answers to frequently asked questions, and learn more about Editorial Manager via interactive tutorials. You can also talk 24/7 to our customer support team by phone and 24/7 by live chat and email

Review 3052022.docx | Bismillah.pdf | Show all

29°C Hujan ringan 14.02 10/05/2022

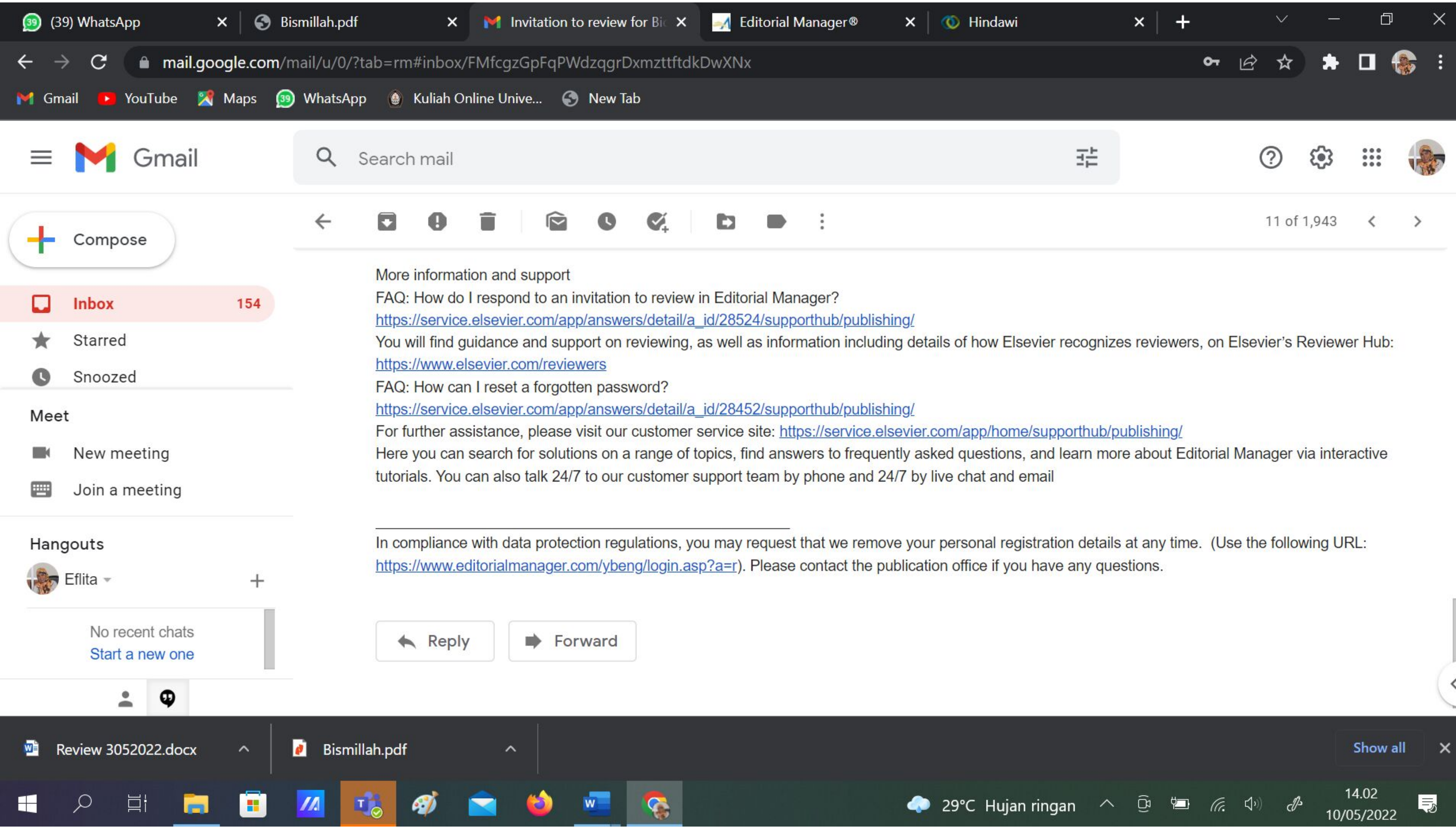

More information and support

FAQ: How do I respond to an invitation to review in Editorial Manager?

https://service.elsevier.com/app/answers/detail/a_id/28524/supporthub/publishing/

You will find guidance and support on reviewing, as well as information including details of how Elsevier recognizes reviewers, on Elsevier's Reviewer Hub:

https://www.elsevier.com/reviewers

FAQ: How can I reset a forgotten password?

https://service.elsevier.com/app/answers/detail/a_id/28452/supporthub/publishing/

For further assistance, please visit our customer service site: https://service.elsevier.com/app/home/supporthub/publishing/

Here you can search for solutions on a range of topics, find answers to frequently asked questions, and learn more about Editorial Manager via interactive tutorials. You can also talk 24/7 to our customer support team by phone and 24/7 by live chat and email

---

In compliance with data protection regulations, you may request that we remove your personal registration details at any time. (Use the following URL: https://www.editorialmanager.com/ybeng/login.asp?a=r). Please contact the publication office if you have any questions.

Reply

Forward

Biosystems Engineering

Numerical simulation for deformation characteristic of tea shoot under negative pressure guidance by the immersed boundary–lattice Boltzmann method

--Manuscript Draft--

Manuscript Number:	YBENG-D-22-00513
Article Type:	Research Paper
Keywords:	famous tea, tea shoot model, negative pressure guidance, IB-LBM
Manuscript Region of Origin:	Asia Pacific

Abstract:	At present, due to the shortage of tea picking labour force, realizing the mechanized picking of famous tea is urgent. Using negative pressure guidance is a feasible method, which can compensate the localization error of machine vision. In this paper, tea shoot with one bud and two leaves is taken as the study object, and a 'Y-type' tea physical model is established according to its physical properties. Moreover, the deformation characteristic of tea shoot under negative pressure guidance is studied by using the immersed boundary–lattice Boltzmann method. The purpose is to analyse the effects of pressure P, vertical deviation H and horizontal deviation W on the deformation characteristics of tea shoot quantitatively. The effectiveness of the numerical calculation method is verified by simulation tests. Results show that P determines fluid velocity, and the difference of steady leaf span (d_s) is small when P is less than 0.990. In addition, setting P = 0.990, when H = 0 and W = 8, d_s achieves a minimum value of 1.78. According to the above findings, this paper provides useful data and insights into the picking technology of famous tea based on negative pressure guidance.

Highlights:

1. A new ‘Y-type’ tea shoot model is established according to the physical properties of tea shoot.
2. The gas–solid two-phase coupling characteristics of tea shoot under negative pressure guidance is studied by using the ‘Y-type’ tea shoot model.

* Corresponding author. E-mail address: jhtong@zstu.edu.cn (Junhua Tong).

Numerical simulation for deformation characteristic of tea shoot under negative pressure guidance by the immersed boundary–lattice Boltzmann method

Yingpeng Zhu[a], Yikun Wei[a,c], Zhengdao Wang[a,c], Rongyang Wang[d], Chuanyu Wu[a,b], Jianneng Chen[a,b], Junhua Tong[a,b,*]

[a] *Faculty of Mechanical Engineering and Automation, Zhejiang Sci-Tech University, 928 Second Avenue, Hangzhou 310018, China*

[b] *Key Laboratory of Transplanting Equipment and Technology of Zhejiang Province, Hangzhou 310018, China*

[c] *National-Provincial Joint Engineering Laboratory for Fluid Transmission System Technology, Hangzhou, 310018, China*

[d] *College of Mechanical and Electrical Engineering, Huzhou Vocational and Technical College, Huzhou 313000, China*

ABSTRACT

At present, due to the shortage of tea picking labour force, realizing the mechanized picking of famous tea is urgent. Using negative pressure guidance is a feasible method, which can compensate the localization error of machine vision. In this paper, tea shoot with one bud and two leaves is taken as the study object, and a 'Y-type' tea physical model is established according to its physical properties. Moreover, the deformation characteristic of tea shoot under negative pressure guidance is studied by using the immersed boundary–lattice Boltzmann method. The purpose is to analyse the effects of pressure P, vertical deviation H and horizontal deviation W on the deformation characteristics of tea shoot quantitatively. The effectiveness of the numerical calculation method is verified by simulation tests. Results show that P determines fluid velocity, and the difference of steady leaf span (d_s) is small when P is less than 0.990. In addition, setting $P = 0.990$, when $H = 0$ and $W = 8$, d_s achieves a minimum value of 1.78. According to the above findings, this paper provides useful data and insights into the picking technology of famous tea based on negative pressure guidance.

Keywords: famous tea, tea shoot model, negative pressure guidance, IB-LBM

1. Introduction

The tea industry is a traditional advantageous business in China, which has played an important role in promoting economic development and rural revitalization. Famous tea has high drinking value and economic benefits, and is an important economic pillar of the tea industry (Wang et al., 2021). At present, the existing tea picking machinery in the world is only suitable for the production of ordinary tea (Han et al., 2019), whereas the famous tea still relies on manual picking. In recent years, a large number of rural labour force has been lost, the picking of famous tea has fallen into labour shortage and the development of tea industry has been seriously restricted (Li et al., 2021). In this predicament, realizing the mechanized picking of famous tea is imperative.

Owing to the different shapes, small size and complex growth environment of tea shoots, accurately obtaining the posture and spatial position of tea shoots with the current identification and location technology is very difficult (Tian et al., 2021). Therefore, picking end effectors are prone to problems, such as picking omission and picking error. At present, relatively few studies on the picking end effector of famous tea are conducted. Qin et al. (2014) developed a picking claw, which is driven by a steering gear, and the intact rate of tea shoots picked was approximately 76.6%. Hao et al. (2018) proposed a bionic picking finger that can imitate the artificial ‘hand-picking’ movement, and the picking success rate in the preliminary indoor test was nearly 70%. Motokura et al. (2020) used a three-finger gripper on the end of the Kinova Jaco robotic arm to complete the tea picking action, but the field test was not carried out. These existing picking end effectors adopt simple mechanical structures, which have insufficient compensation ability for localization error, resulting in low picking success rate and intact rate of tea shoots. In response to this problem, a tea shoot picking method based on negative pressure guidance was proposed (Zhu et al., 2021). The principle is to guide the tea shoot into a pipe through negative pressure and then cut the tea shoot. This method involves the scientific field of gas–solid two-phase flow.

Gas–solid two-phase flow is one of the frontier problems in agriculture and has been widely applied in agricultural production, such as pneumatic seeding (Han et al., 2018), pneumatic fertilization (Zheng et al., 2019), pneumatic screening (Ma et al., 2019) and pneumatic conveying (Kuang et al., 2018). Accurately predicting the deformation characteristics and motion trajectories of agricultural materials in multiphase flow is of great importance to the development of agricultural machinery. At present, relevant studies mainly focus on near-spherical agricultural materials such as droplet spray (Zhu et al., 2019) and seed (Guzman et al., 2020). To reduce complexity, near-spherical materials are usually simplified as spherical particles, and then the commercial software of computational fluid dynamics (CFD) and the discrete element method are used for numerical calculation. This method is difficult to apply to tea because tea is a flexible, flaky material, and the spheroidization treatment may lead to large calculation errors.

The immersed boundary–lattice Boltzmann method (IB-LBM) has the advantages of scalability, parallel computing, high model accuracy and calculation efficiency, and is regarded an effective alternative to traditional CFD in calculating material deformation and movement (Xiong et al., 2019; Tao et al., 2019;). Many studies have shown that the IB-LBM method has unique advantages in the gas–solid coupling numerical computation of flexible material, such as filament (Wang et al., 2018), flag (Wang et al., 2019a) and flake plate (Tang et al., 2016). At present, the application of the IB-LBM method in the field of tea is rarely reported. Wang et al. (2019b) used the IB-LBM method to study the fluid–structure coupling technology between tea and viscous fluid. The tea was simplified to a circle and assumed elliptical after deformation. The motion trajectories and deformation characteristics of tea in the air flow were numerically calculated. In the study of tea sorting, simplifying tea into a circle is feasible, but to study the deformation characteristics of a single tea shoot, establishing a new tea shoot model for more specific tea shoot morphology is necessary.

In this paper, a 'Y-type' tea shoot model is established according to the physical characteristics of tea shoot, and the gas–solid two-phase coupling characteristics of tea shoot under negative pressure guidance is studied by using the IB-LBM method. The purpose is to clarify the mechanism of negative pressure guidance, which can be used to guide and optimize the design of picking end effector. This paper has important theoretical importance and application value for the development of picking end effector with high success rate, low damage and good deviation tolerance performance, and can provide reference for other similar pneumatic picking equipment.

The remainder of this paper is organized as follows. In Section 2, the numerical method, tea shoot model and boundary conditions are briefly introduced. In Section 3, the detailed results of numerical simulation are presented, and the effects of pressure and position deviation on the deformation of tea shoot are discussed. Finally, the main conclusions of this paper are given in Section 4, and the future study is discussed.

2. Numerical method for deformation of tea shoot

2.1. Immersed boundary–lattice Boltzmann method

In this paper, the code based on IB-LBM is developed. The basic idea of IB-LBM is solving two equation systems: lattice Boltzmann evaluation system on Eulerian fluid points and artificial correction system on Lagrangian boundary points. The lattice Boltzmann evaluation system is solved by lattice Boltzmann equation (Wu et al., 1992), which can be written as

$$f_\alpha(\mathbf{x}+\mathbf{e}_\alpha\delta_t, t+\delta_t) = f_\alpha(\mathbf{x},t) - \frac{1}{\tau}\left[f_\alpha(\mathbf{x},t) - f_\alpha^{eq}(\mathbf{x},t)\right] + F_\alpha\delta_t, \tag{1}$$

where f_α is the density distribution function at direction $\mathbf{e}_\alpha$, $\mathbf{e}_\alpha$ is the discretized velocity, $\mathbf{x}$ is the fluid point, δ_t is the time interval, τ is the single relaxation parameter, f_α^{eq} is the equilibrium function and

F_α is the discrete force term. In the commonly used D2Q9 model (Qian et al., 1992), $\mathbf{e}_\alpha$ is given as

$$\mathbf{e}_\alpha = \frac{\delta x}{\delta t}\begin{bmatrix} 0 & 1 & 0 & -1 & 0 & 1 & -1 & -1 & 1 \\ 0 & 0 & 1 & 0 & -1 & 1 & 1 & -1 & -1 \end{bmatrix}. \tag{2}$$

The equilibrium function is given as

$$f_\alpha^{eq} = \rho w_\alpha \left[1 + \frac{\mathbf{e}_\alpha \cdot \mathbf{u}}{c_s^2} + \frac{(\mathbf{e}_\alpha \cdot \mathbf{u})^2}{2c_s^4} + \frac{\mathbf{u}\cdot\mathbf{u}}{2c_s^2}\right], \tag{3}$$

where w_α is the weight coefficients, and c_s is the speed of sound. Parameters in D2Q9 model are given as

$$c_s = \frac{1}{\sqrt{3}}\frac{\delta x}{\delta t}, w_\alpha = \begin{cases} \frac{4}{9} & \alpha = 0, \\ \frac{1}{9} & \alpha = 1 \sim 4. \\ \frac{1}{36} & \alpha = 5 \sim 8 \end{cases} \tag{4}$$

The relation between single relaxation parameter τ and kinematic viscosity ν is

$$\nu = (\tau - 0.5)c_s^2\delta_t. \tag{5}$$

A commonly used discrete force term proposed by Guo (Guo et al., 2002) is given as

$$F_\alpha = \left(1 - \frac{1}{2\tau}\right) w_\alpha \left[\frac{\mathbf{e}_\alpha - \mathbf{u}}{c_s^2} + \frac{\mathbf{e}_\alpha \cdot \mathbf{u}}{c_s^4}\mathbf{e}_\alpha\right] \cdot \mathbf{f}_\alpha(\mathbf{x}, t). \tag{6}$$

In this mesoscopic system, the macroscopic variables, local density, velocity and pressure can be calculated by

$$\rho = \sum_\alpha f_\alpha, \tag{7}$$

$$\mathbf{u} = \frac{1}{\rho}\left(\sum_\alpha \mathbf{e}_\alpha f_\alpha + \frac{1}{2}\mathbf{f}\delta_t\right), \tag{8}$$

$$p = c_s^2 \rho. \tag{9}$$

The artificial correction system is solved by coupling equation, and the schematic diagram of the immersed boundary method is shown in Fig. 1.

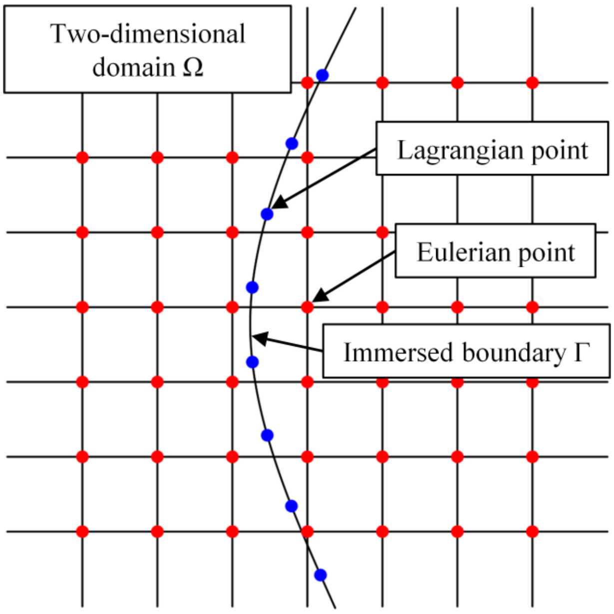

Fig. 1 Schematic diagram of immersed boundary method

The force density of the Eulerian point is calculated from the force density of the Lagrangian point by Eq. (11). Similarly, the velocity of the Lagrangian point on the immersed boundary is updated based on the velocity of Eulerian point, as shown in Eq. (12).

$$\mathbf{f}(\mathbf{x},t)=\int_{\Gamma}\mathbf{F}(s,t)\delta(\mathbf{x}-\mathbf{X}(s,t))ds, \tag{11}$$

$$\mathbf{U}(s,t)=\mathbf{u}(\mathbf{X}(s,t),t)=\frac{\partial\mathbf{X}(s,t)}{\partial t}=\int_{\Omega}\mathbf{u}(\mathbf{x},t)\delta(\mathbf{x}-\mathbf{X}(s,t))d\mathbf{x}, \tag{12}$$

where $\mathbf{f}(\mathbf{x},t)$ is the force density of the Eulerian point, $\mathbf{F}(s,t)$ is the boundary force density of the Lagrangian point, $\mathbf{U}(s,t)$ is the velocity of a Lagrangian point and $\mathbf{u}(\mathbf{x},t)$ is the fluid velocity of the Eulerian point. The velocity density or density distribution function at Lagrangian position can be obtained from Eulerian points by using Dirac delta function.

$$\delta(\mathbf{x})=\delta(x)\cdot\delta(y), \tag{13}$$

where $\delta(x)$ is defined as

$$\delta(r)=\begin{cases}\frac{1}{4}\left(1+\cos\left(\frac{\pi|r|}{2}\right)\right) & |r|<2\\ 0 & |r|\geq 2\end{cases}. \tag{14}$$

2.2. Method for tea shoot model established

Fig. 2(a) shows that the study object is a tea shoot with one bud and two leaves. To explore the deformation law of tea shoot under negative pressure guidance, a ‘Y-type’ tea shoot model is established, as shown in Fig. 2(b), according to the physical characteristics of tea shoot. The tips of the first leaf (FL) and the second leaf (SL) are marked as Q_1 and Q_2, respectively. The nodes of FL and SL are marked as

Q_3 and Q_4, respectively. The horizontal spacing between Q_1 and Q_2 is defined as leaf span d. Moreover, θ_{10} is the initial included angle between FL and the vertical direction, θ_{20} is the initial included angle between SL and the vertical direction and $\theta_{10} = -30°$and $\theta_{20} = 30°$. Under negative pressure guidance, FL and SL rotate around Q_3 and Q_4, respectively, but the bending deformation is very small. Therefore, in this paper, the FL and SL of the tea shoot model are defined as rigid bodies, and the deformed tea shoot model is shown in Fig. 2(c). θ_1 is the included angle between FL and the vertical direction in the current time step. θ_2 is the included angle between SL and the vertical direction in the current time step.

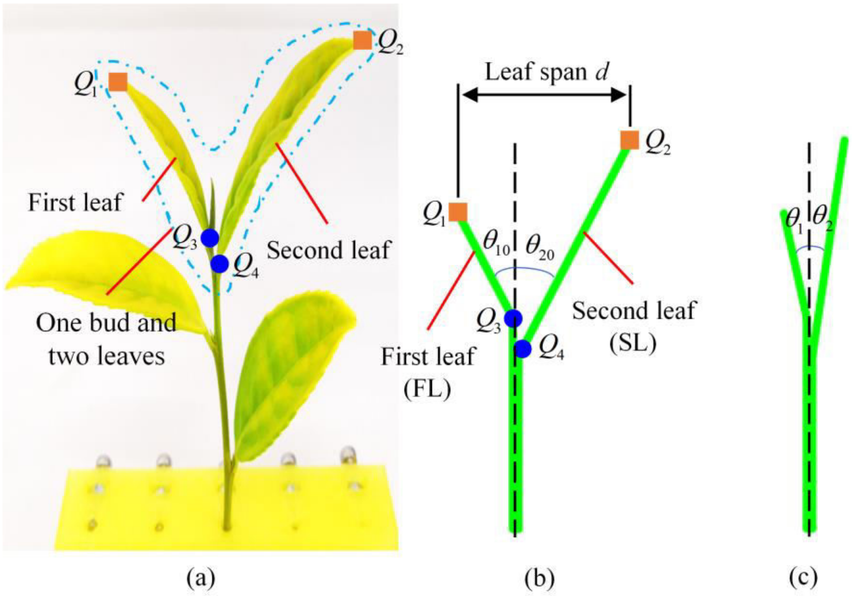

Fig. 2. Schematic diagram of tea shoot model: (a) fresh tea shoot, (b) tea shoot model before deformation, (c) deformed tea shoot model

In this paper, the functional expression of the tea shoot model is given. The ‘Y-type’ tea shoot model is discretized into N particles, and the x–y coordinate expression of the nth particle is shown in Eqs. (15) and (16).

$$x = \begin{cases} x_0 - \frac{1}{2}\left(n - \frac{N}{3}\right)\sin\theta_{20}, & 0 \le n < \frac{N}{3} - 1 \\ x_0 + \frac{1}{4}, & \frac{N}{3} - 1 \le n < \frac{N}{2} + 7 \\ x_0 - \frac{1}{4}, & \frac{N}{2} + 7 \le n < \frac{5N}{6} \\ x_0 + \frac{1}{2}\left(n - \frac{5N}{6} + 1\right)\sin\theta_{10}, & \frac{5N}{6} \le n < N \end{cases}, \tag{15}$$

$$y=\begin{cases} y_0-\frac{1}{2}\left(n-\frac{N}{3}\right)\cos\theta_{20}, & 0\le n<\frac{N}{3}-1 \\ y_0-\frac{1}{2}\left(n-\frac{N}{3}-\cos\theta_{20}+1\right), & \frac{N}{3}-1\le n<\frac{N}{2}+7 \\ y_0+\frac{1}{2}\left(n-\frac{5N}{6}+\cos\theta_{10}\right)+3, & \frac{N}{2}+7\le n<\frac{5N}{6} \\ y_0+\frac{1}{2}\left(n-\frac{5N}{6}+1\right)\cos\theta_{10}+3, & \frac{5N}{6}\le n<N \end{cases}, \tag{16}$$

where (x_0, y_0) is the centre of the tea shoot model (tea centre), $0 \le n < N/3-1$ indicates the particle is on SL, $5N/6 \le n < N$ indicates the particle is on FL and the rest indicates the particle is on the stem.

Under the driven fluid, the total torque T_1 of the particles on FL and total torque T_2 of the particles on SL are defined as

$$T_1=\sum_{n=\frac{5}{6}N+1}^{N-1}\frac{1}{2}\left(f_y\cdot\sin\theta_1-f_x\cdot\cos\theta_1\right)\left(n-\frac{5}{6}N\right), \tag{17}$$

$$T_2=\sum_{n=0}^{\frac{N}{3}-2}\frac{1}{2}\left(f_y\cdot\sin\theta_2-f_x\cdot\cos\theta_2\right)\left(\frac{N}{3}-1-n\right). \tag{18}$$

where f_x and f_y are the forces in the x and y directions given by the fluid to the particles, respectively. Reset torque T_3 on FL node and reset torque T_4 on SL node are defined as

$$T_3=k_1\left(\theta_1-\theta_{10}\right), \tag{19}$$

$$T_4=k_2\left(\theta_2-\theta_{20}\right), \tag{20}$$

where k_1 and k_2 are the rotational stiffness of FL and SL, respectively; $k_1 = 0.04$ and $k_2 = 0.12$. Moreover, the angular velocity ω_1 of FL and the angular velocity ω_2 of SL can calculated by Eqs. (21) and (22), respectively.

$$\omega_1=\frac{T_1+T_3}{J_1}\delta t, \tag{21}$$

$$\omega_2=\frac{T_2+T_4}{J_2}\delta t, \tag{22}$$

where J_1 and J_2 are the rotational inertia of FL and SL, respectively. The calculation results can be used to update the tea position of the next time step.

2.3. Boundary and initial conditions

Fig. 3 illustrates the negative pressure guidance scheme and computational domain, the computational grid consists of 300 × 300 points and the tea shoot model is placed at the centre of the computational domain. A negative pressure guide pipe with an inner diameter of 15 and a length of 100 is arranged at the top of the flow field. (153,178) is selected as the reference point because it is on the central axis of the negative pressure guiding pipe and close to the pipe mouth whilst ensuring that the tea does not touch the pipe.

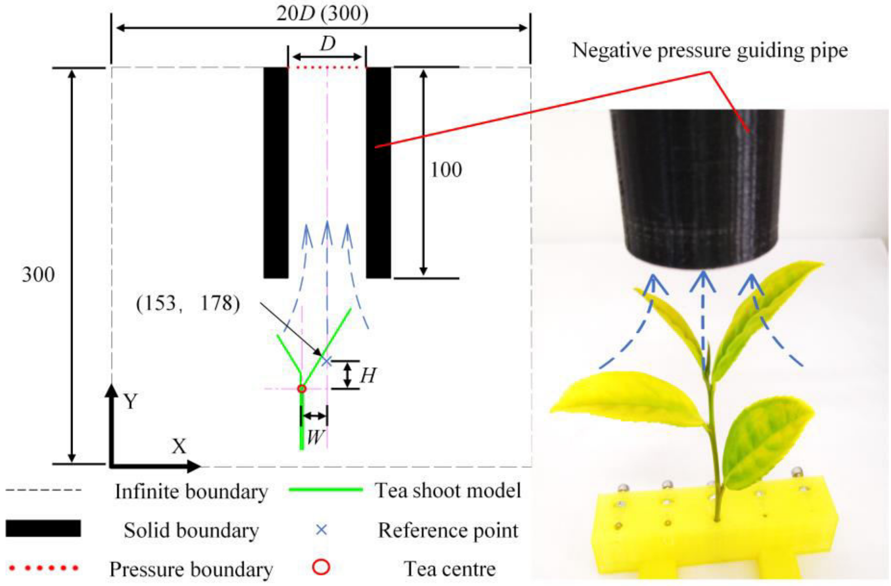

Fig. 3. Computational domain and boundary conditions in the 2D domain

The horizontal and vertical deviations between the tea centre and the reference point are *W* and *H*, respectively. *W* and *H* are defined as

$$W = x_{tea\ centre} - x_{reference\ point}, H = y_{tea\ centre} - y_{reference\ point}. \quad (23)$$

In this paper, the bounce-back scheme, the nonequilibrium extrapolation scheme and the immersed boundary method are applied. The bounce-back scheme is executed for the solid boundary. The idea of bounce-back scheme is expressed by the following expressions.

$$f'_{\bar{\alpha}}\left(\mathbf{x}_{sf}, t+\delta t\right) = f_{\alpha}\left(\mathbf{x}_{sf}, t+\delta t\right), \quad (24)$$

$$\alpha = \left[0,1,2,3,4,5,6,7,8\right], \bar{\alpha} = \left[0,3,4,1,2,7,8,5,6\right], \quad (25)$$

where f'_{α} is the density distribution function after collision, and $\mathbf{x}_{sf}$ is fluid point around the solid boundary.

The nonequilibrium extrapolation scheme is executed for the pressure boundary and the infinite boundary. The idea of nonequilibrium extrapolation scheme boundary is expressed by the following expressions.

$$f_{\alpha}(\mathbf{x}_b, t) = f_{\alpha}^{eq}(\rho_b, u_{bf}) + \left[f_{\alpha}(\mathbf{x}_{bf}, t) - f_{\alpha}^{eq}(\rho_{bf}, u_{bf})\right], \quad (26)$$

where $\mathbf{x}_b$ is the point on the pressure boundary or the infinite boundary; ρ_b is the density of $\mathbf{x}_b$; $\mathbf{x}_{bf}$ is the fluid point next to $\mathbf{x}_b$ along the boundary normal vector; ρ_{bf} and u_{bf} are the density and velocity of $\mathbf{x}_{bf}$, respectively.

The immersed boundary method is used to solve the coupling problem between the tea shoot model and the fluid. The external force of the fluid point and the velocity of the Lagrange point on the tea shoot model can be updated through Eqs. (11) and (12), respectively.

2.4. Simulation test scheme

To study the effects of pressure P and position deviation (*H* and *W*) on the deformation of tea shoot, 41 groups of simulation tests are conducted, and 100,000 steps are calculated for each group. During calculation, the overall data are recorded once every 1,000 steps, which includes leaf span *d*, x coordinates of Q_1 and Q_2 (X_1 and X_2, respectively), half-life period *T*, velocity and vorticity of fluid. *d* reflects the deformation degree, and *T* reflects the deformation efficiency. Moreover, d_f is defined as the *d* at step 100,000 (final leaf span), and d_s is defined as the *d* in stable state (steady leaf span). In addition, to study the fluid–tea interaction, the final velocity of fluid points on three sets of horizontal lines (A, B and C) expressed in Eq. (27) are counted. Finally, most current studies based on IB-LBM are dimensionless (Wang et al., 2022). Therefore, to simplify the calculation, the above parameters are also dimensionless and will be dimensionalized in future study.

$$\begin{cases} y_A = y_{tea\ centre} + 15 & 125 \le x_1 \le 181 \\ y_B = y_{tea\ centre} + 10 & 125 \le x_2 \le 181. \\ y_C = y_{tea\ centre} + 5 & 125 \le x_3 \le 181 \end{cases} \tag{27}$$

Fig. 4 illustrates the simulation scheme for studying the effect of *P*. During the simulation, the tea centre is located at the reference point (153,178), and *P* is set to decrease from 0.999 to 0.984 with a decrement of 0.003, that is, six simulation tests are carried out.

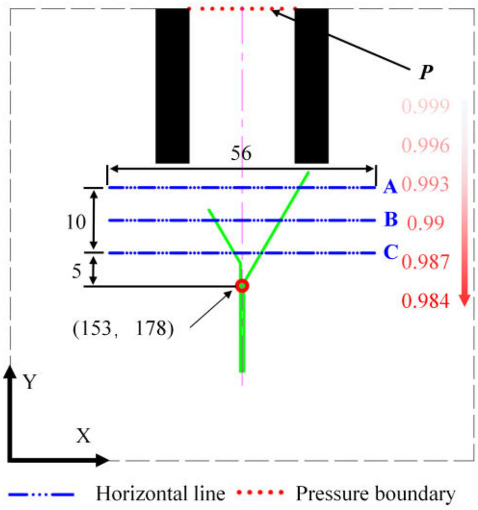

Fig. 4. Schematic diagram of simulation scheme for studying the effect of *P*

To explore the effects of horizontal deviation *W* and vertical deviation *H* on the deformation of tea shoot, a simulation scheme is developed, as shown in Fig. 5. The uniformly distributed blue point is the test point, and the distance between adjacent points is 4. In the simulation, the pressure *P* is set to 0.990, and 36 simulation tests are conducted. The setting of pressure P is based on that when P is less than 0.990 and continues to decrease. The total deformation of tea has a minimal difference.

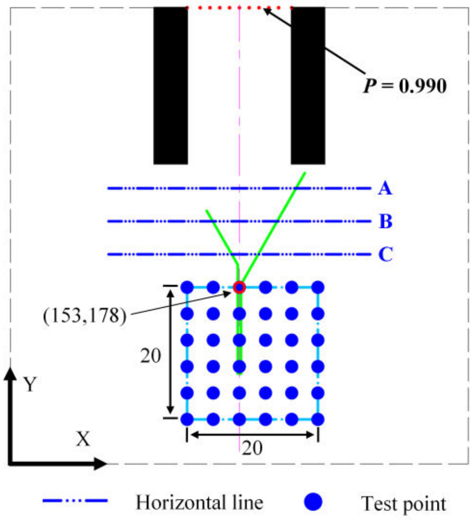

Fig. 5. Schematic diagram of simulation scheme for studying the effects of W and H

3. Results and discussions

In this section, the deformation of tea shoot is shown by discussing the details of velocity and vorticity of fluid. In addition, the effects of a single factor (P or H or W) and multiple factors (H and W) on the deformation of tea shoot are clarified.

3.1. Effect of pressure P on deformation of tea shoot

3.1.1. Time evolution of velocity, vorticity and tea shoot under different pressures

Fig. 6(a) shows the time evolution of velocity, vorticity and tea shoot at $P = 0.984$. Fig. 6(a1) shows that in the initial period, two flow channels are in the flow field, and the left flow channel is remarkably larger than the right flow channel. Moreover, some vortices are formed near the pipe mouth and tea shoot, amongst which the positive vortex at Q_1 and the negative vortex at the left side of the pipe mouth are larger. Fig. 6(a2) shows that under negative pressure guidance, the velocity of airflow in the pipe increases, and FL and SL gradually rotate towards the centre of the pipe mouth. Furthermore, the positive vortex at Q_1 extends and merges with the positive vortex at the right side of the pipe mouth. Fig. 6(a3) shows that SL continues to rotate, and the positive vortex at the left of SL merges with the positive vortex at the right side of the pipe mouth. Fig. 6(a4) shows the final calculation results. At this time, the rotation angle of FL is smaller than that of SL. However, due to the large rotation angle of SL, the distance between SL and the right side of the pipe mouth increases, making the right flow channel evident, and the size of the vortices near the flow channels on both sides is approximate. Moreover, in the left flow channel, the vorticity of the positive vortex at Q_1 decreases, whereas the vorticity of the positive vortex at Q_2 increases.

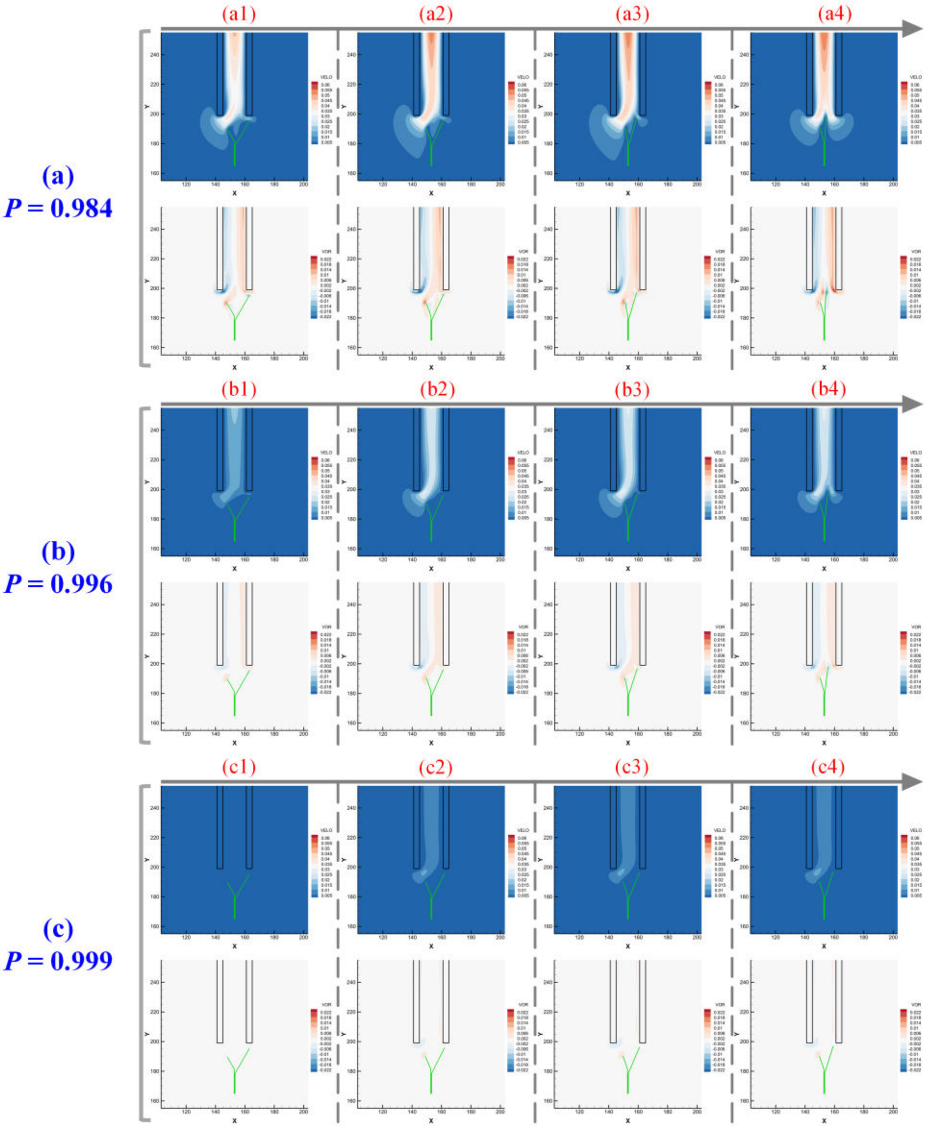

Fig. 6. Time evolution of velocity, vorticity and tea shoot under different pressures: (a) $P = 0.984$, (b) $P = 0.996$, (c) $P = 0.999$

Fig. 6(b) illustrates the time evolution of velocity, vorticity and tea shoot at $P = 0.996$. Velocity and vorticity are less than those at $P = 0.984$. Fig. 6(b1) shows that the right flow channel is not evident. Moreover, a positive vortex is formed at Q_1, and a negative vortex is formed at Q_2. Similar to Fig. 6(a2), in Fig. 6(b2), the velocity of airflow in the pipe increases, and d gradually decreases. In addition, the positive vortex at Q_1 merges with the positive vortex at the right side of the pipe mouth, and a new negative vortex is generated at the right side of Q_1. Fig. 6(b3) shows that as SL continues to rotate, the positive vortex between Q_1 and the right side of pipe mouth extends towards Q_2. Fig. 6(b4) shows that in the final state, SL has a large rotation angle, and the right flow channel appears. Compared with Fig. 6(a4), in addition to the smaller velocity and vorticity, d_f becomes larger.

Fig. 6(c) describes the time evolution of velocity, vorticity and tea shoot at P = 0.999. Its velocity and vorticity are very small. Fig. 6(c1) shows that observing the flow phenomenon is difficult, and only a small negative vortex appears at the left side of the pipe mouth. Fig. 6(c2) shows only the left flow channel. The negative vortex at the left side of the pipe mouth expands, and a positive vortex is formed at Q_1. The difference between Figs. 6(c2)–6(c4) is mainly reflected in the morphological changes of tea, and no evident difference in velocity and vorticity is observed. Comparing the deformation of tea shoot in Figs. 6(a4) and 6(b4) shows that the d_f in Fig. 6(c4) is larger.

Based on the above analysis, with the decrease of P, fluid velocity increases, making the final deformation of tea shoot larger. Comparing the deformation of tea shoot under these three pressures, the effect of decreasing pressure on the deformation of tea shoot decreases gradually.

3.1.2. Velocity distribution under different pressures

To analyse the fluid–tea coupling properties, exploring the velocity distribution of the fluid around the tea shoot is necessary. Fig. 7 shows the final velocity of fluid points on three groups of horizontal lines (A, B and C) under six different pressures, and Fig. 4 shows the horizontal lines (A, B and C). Waveform comparison reveals that the trends of the polylines in Figs. 7(b)–7(f) are similar, mainly showing two mountains and one valley, in which the left peak is higher than the right peak. The reason is that the gap between SL and the pipe mouth is relatively small, which hinders the inflow of air, causing the fluid velocity on the left side of the tea to be higher than that on the right side at the same horizontal line. Furthermore, the right peak of the polyline in Fig. 7(a) is not substantial. The reason is that as shown in Fig. 6(c), the gap between SL and the right side of the pipe mouth is very small, which limits the entry of airflow. Therefore, the velocity of the fluid point on the right side of tea shoot is very small, which is reflected in that when X $\geq$ 160, the velocity U of the fluid point on the three groups of horizontal lines is close to zero. With the decrease of P, the gap between SL and the right side of the pipe mouth increases gradually, which makes more air flow into the pipe from the right side of the tea. Therefore, the fluid velocity on the right side of the tea gradually increases, which is reflected in the fact that the right peak of the polyline begins to highlight. The overall trend displays that when pressure is constant, the closer the horizontal line is to the pipe mouth, the greater the average velocity of the fluid point. For the same horizontal line, the lower the pressure is, the greater the average velocity of the fluid point.

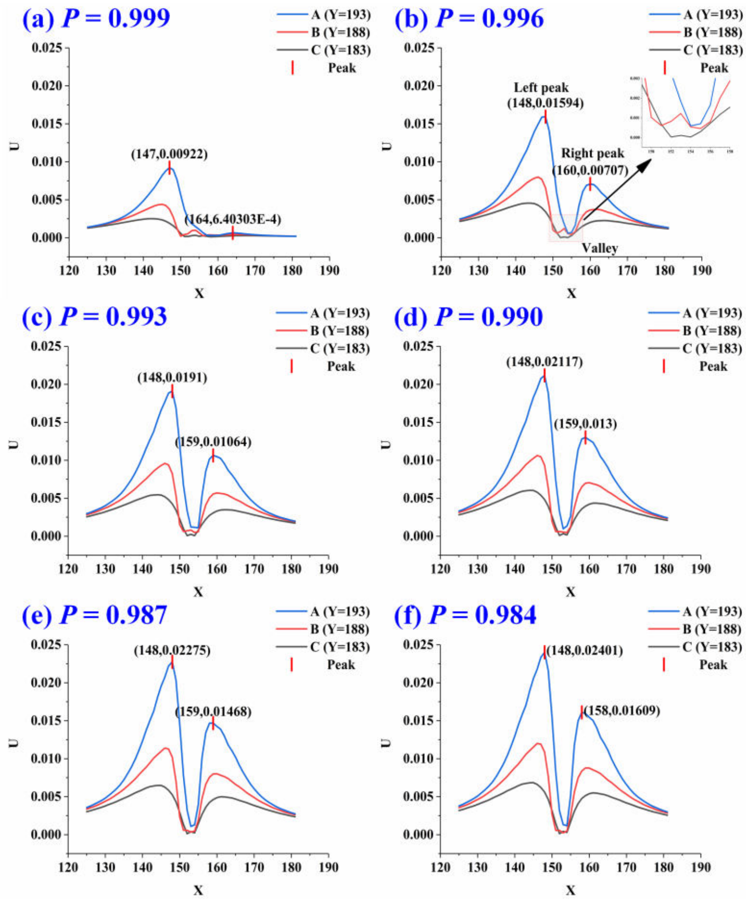

Fig. 7 Velocity distribution on three groups of horizontal lines (A, B and C) under different pressures: (a) P = 0.999, (b) P = 0.996, (c) P = 0.993, (d) P = 0.990, (e) P = 0.987, (f) P = 0.984

Taking the velocity polyline corresponding to A as an example, data analysis exhibits that P is negatively correlated to the increment of velocity peak value. When P decreases from 0.999 to 0.996, the left peak value increases from 0.00922 to 0.01594 with an increment of 0.00672, and the right peak value increases from 0.00064 to 0.00707 with an increment of 0.00643. However, when P decreases from 0.987 to 0.984, the left peak value increases from 0.02275 to 0.02401 with an increment decreasing to 0.00126, which is 18.75% of the original increment. The right peak value increases from 0.01468 to 0.01609 with an increment of 0.00141, which is 21.93% of the original increment. In addition, the ratio of the left peak value to right peak value is defined as i, and P is also positively correlated to i. When P = 0.999, i is 14.45, and when P = 0.984, i decreases to 1.49.

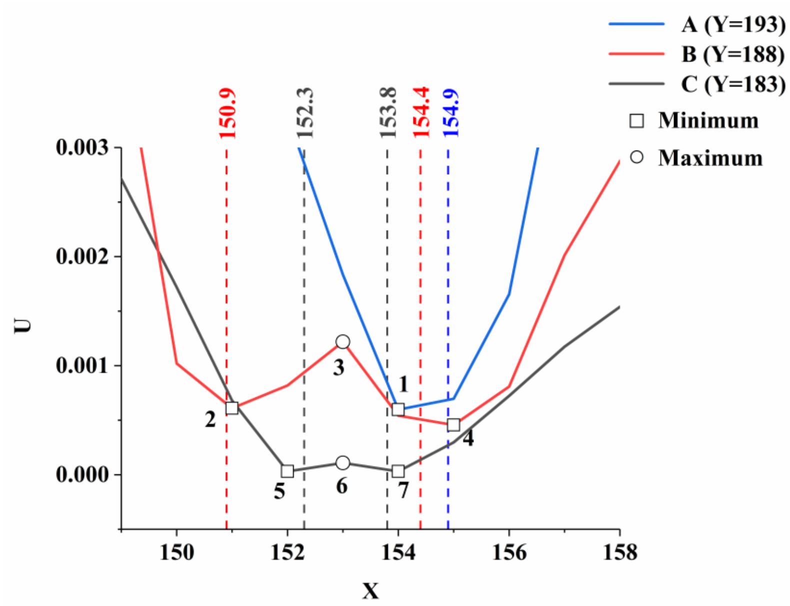

Fig. 8. Schematic diagram of valley in Fig. 7(b)

The velocity of the surrounding fluid point is very low due to the blocking effect of tea, so a valley is in the polyline. When the position of the tea centre remains unchanged, its own deformation is the main factor affecting the position of the valley. Taking P = 0.996 as an example, the valley in Fig. 7(b) is shown in Fig. 8. The valley in the polylines corresponding to B and C have one maximum (points 3 and 6) and two minimums (points 2, 4, 5 and 7). However, the valley in the polyline corresponding to A has only one minimum value (point 1), which is caused by the different positional relationship between the three sets of horizontal lines and the tea leaves. Figs. 4 and 8 show that the tea shoot model is 'Y-type'. The horizontal line C intersects FL and SL, and the x coordinates of the intersection point are 152.3 and 153.8, respectively. Therefore, the minimum values appear near the intersection point, which are points 5 and 7. However, fluid point remains between the two points, which are relatively largely affected by the peripheral airflow, resulting in a maximum point 6. The horizontal line B also intersects with FL and SL, and the x coordinates of the intersection point are 150.9 and 154.4, respectively. Therefore, the minimum values appear near the intersection point, which are points 2 and 4. Moreover, fluid points with large velocity are between the two points, resulting in a maximum point 3. The horizontal line A only intersects with SL, and the x coordinate of the intersection point is 154.9. Therefore, the minimum value appears near the intersection point, which is point 1. The above analysis of the valley will not be repeated later due to the same principle.

3.1.3. Temporal evolution of tea span and leaf tip x coordinates under different pressures

To reflect the deformation of tea intuitively, the time evolution of tea span and leaf tip x coordinates under six different pressures are drawn, as shown in Fig. 9. Figs. 9(a)–9(f) illustrate that when pressure remains unchanged, with the passage of time, X_1 increases first and then decreases, and X_2 gradually decreases, which together lead to the decrease of the d. The reason for the decrease of X_1 is that the flow velocity of the fluid around FL is reduced due to the enlargement of the right flow channel. In addition, over time, the deformation amount of the same time interval becomes smaller, and tea gradually stabilizes. Figs. 9(b)–9(f) show that after 100,000 steps of calculation, the three parameters (d, X_1 and X_2) remain unchanged, indicating that the flow field has reached a stable state and the deformation of tea shoot has ended. At this time, d is a stable value, which means $d_f = d_s$. However, Fig. 9(a) shows that the flow field has not reached a stable state after 100,000 steps of calculation, and d_s needs to be calculated through linear fitting. Considering the overall trend, the pressure decreases, d_f becomes smaller and the deformation speed becomes faster.

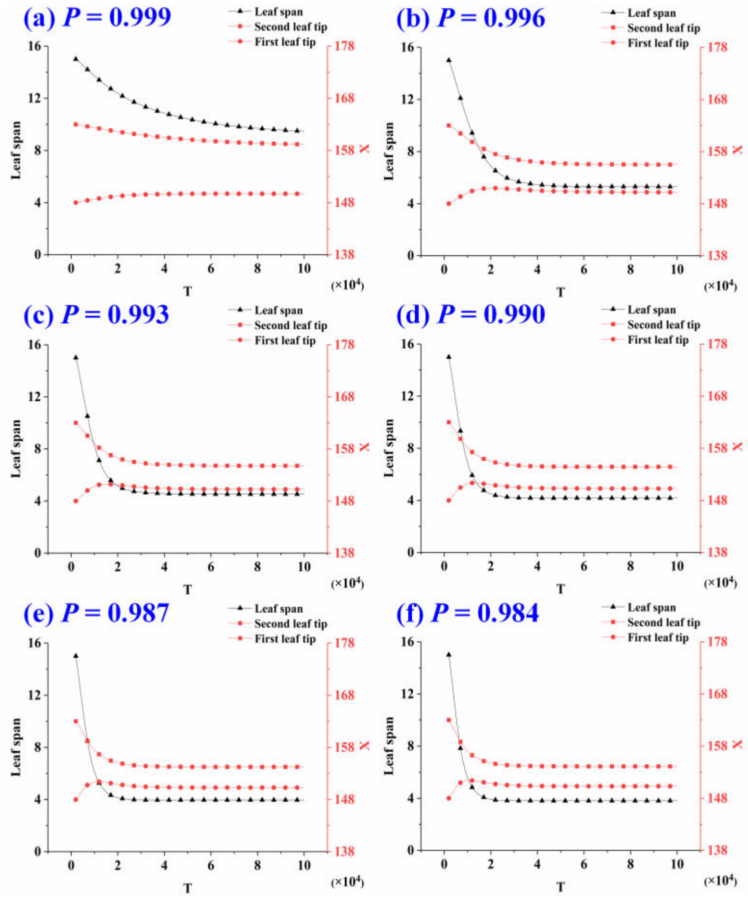

Fig. 9. Temporal evolution of tea span and leaf tip x coordinates under different pressures: (a) P = 0.999, (b) P = 0.996, (c) P = 0.993, (d) P = 0.990, (e) P = 0.987, (f) P = 0.984

To analyse the relationship between P and d_s quantitatively, the polyline of d_s changing with P is plotted, as presented in Fig. 10. The decrement of d_s is smaller. When pressure P decreases from 0.999 to 0.996, the decrement of d_s is 5.8. However, when P decreases from 0.987 to 0.984, the decrement of d_s decreases to 0.15. This phenomenon has two main reasons. Firstly, FL is far from the pipe mouth, so it is less affected by pressure. Therefore, the velocity increment of the fluid at this position is small, resulting in the small rotation angle increment of FL. Secondly, the rotation angle of SL is large, which is approximately vertical. The increment of torque provided by the fluid becomes smaller, so the rotation angle increment of SL also becomes smaller.

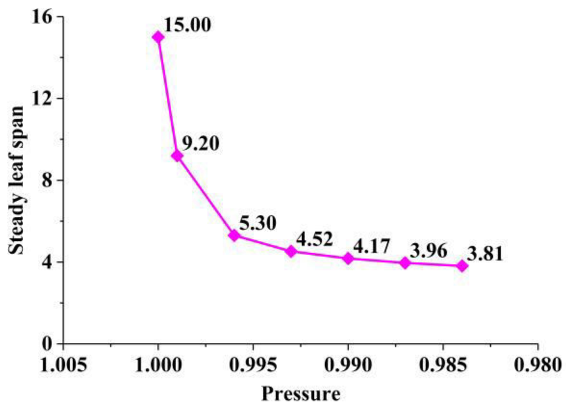

Fig. 10. Steady leaf span changing with pressure

To explore the relationship between P and T, a polyline of T changing with P is drawn. Fig. 11 shows that with the decrease of P, T is gradually shortened. It means that the smaller the P is, the higher the deformation efficiency of tea shoot. T is 23,394 at $P = 0.999$, which indicates that under this condition, 23,394 steps need to be calculated for every 50% decay of d. However, when $P = 0.984$, T decreases to 2,177, which is only 9.3% of the former.

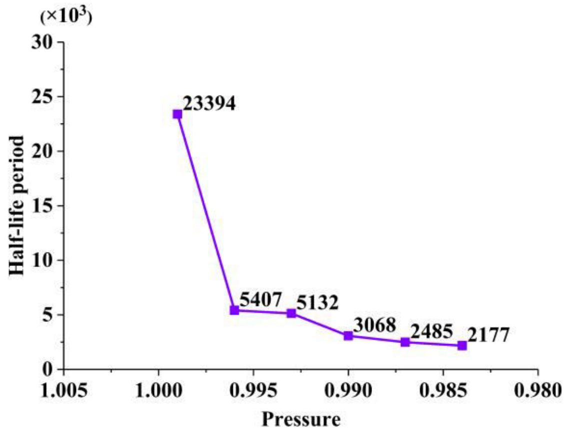

Fig. 11. Half-life period changing with pressure

3.2. Effect of vertical deviation H on deformation of tea shoot

3.2.1. Time evolution of velocity, vorticity and tea shoot under different vertical deviations

Fig. 12(a) illustrates the time evolution of velocity, vorticity and tea shoot at $H = -20$. Fig. 12(a1) shows only one flow channel in the flow field, and a negative vortex and a positive vortex appear at the left and right sides of the pipe mouth, respectively. Moreover, the velocity of the fluid around tea shoot is extremely small, and only a small negative vortex is found at Q_2 around the tea. However, as described in Fig. 12(a2), the negative vortex at the second tip disappears over time. Comparison reveals no remarkable difference in velocity, vorticity and tea shoot in Figs. 12(a2)–12(a4), which indicates that when H is small, fluid has a minimal effect on tea.

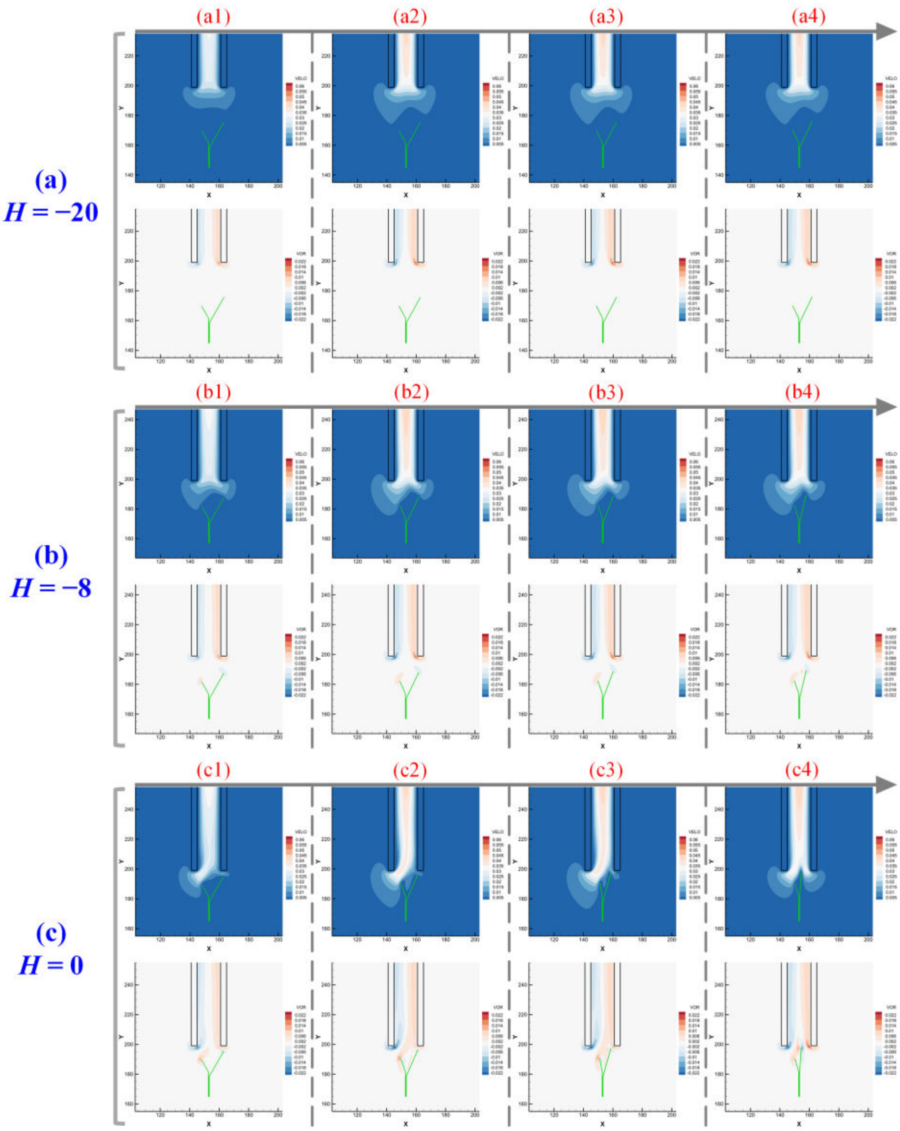

Fig. 12. Time evolution of velocity, vorticity and tea shoot under different vertical deviations: (a) $H = -20$, (b) $H = -8$, (c) $H = 0$

Fig. 12(b) describes the time evolution of velocity, vorticity and tea shoot at $H = -8$. Fig. 12(b1) shows two evident flow channels in the flow field, and the left flow channel is larger than the right flow channel. In addition, a positive vortex is formed at Q_1, and a negative vortex is formed at Q_2. Fig. 12(b2) shows that over time, the velocity of the fluid in the pipe increases, and the vorticity of the vortex at the pipe mouth increases. In addition, d decreases, and the size of the positive vortex at Q_1 increases. Fig. 12(b3) shows that FL and SL continue to rotate towards the middle, and the negative vortex at Q_2 extends outward. In the final state, SL continues to rotate to the middle, and the rotation angle of FL is very small in comparison, as shown in Fig. 12(b4). Furthermore, a positive vortex is formed at the left side of Q_2. Compared with Fig. 12(a4), d_f is smaller.

Fig. 12(c) shows the time evolution of velocity, vorticity and tea shoot at $H = 0$. At this time, the tea is at the reference point. Fig. 12(c1) shows that in the initial period, the right flow channel is small. A positive vortex and a negative vortex appear at the left and right sides of Q_1, respectively. Moreover, the positive vortex is clearly greater than the negative vortex. Similar to Fig. 6(a), as shown in Fig. 12(c2), the positive vortex at Q_1 extends outward and merges with the positive vortex at the right side of the pipe mouth. In addition, the positive vortices appear at the left side of SL. In Fig. 12(c3), the positive vortices at the left side of SL also merge with the positive vortex at the right side of the pipe mouth. Fig. 12(c4) shows that the right flow channel becomes larger, the fusion of these vortices is destroyed and the vorticity of the vortices at Q_2 increases. In addition, the deformation of tea shoot is greater than that in Fig. 12(b4).

In summary, with the increase of H, the velocity and vorticity of the fluid around tea shoot gradually increase, and d_f decreases.

3.2.2. Velocity distribution under different vertical deviations

To analyse the relationship between the velocity of the fluid around the tea and the deformation of tea shoot further, Fig. 13 is plotted. It shows the final velocity of fluid points on three groups of horizontal lines (A, B and C) under six different vertical deviations, and the horizontal lines (A, B and C) are expressed as Eq. (27).

Waveform comparison clearly shows that the trends of the polylines in Figs. 13(a)–13(f) are similar, mainly showing two mountains and one valley, in which the left peak is higher than the right peak. Moreover, with the increase of H, the valley of the velocity polyline becomes narrower. The main reason is that when H increases, d_f decreases, and the area blocked by tea shoot on the horizontal line shrinks. Finally, considering the overall trend, for the same horizontal line, the greater the vertical deviation H is, the greater the average velocity of the fluid point.

Taking the velocity polyline corresponding to A as an example, data analysis reveals that H is positively correlated with the increment of velocity peak value. When H increases from −20 to −16, the left peak value increases from 0.00477 to 0.00616 with an increment of 0.00139, and the right peak value increases from 0.00267 to 0.00308 with an increment of 0.00041. However, when H increases from −4 to 0, the left peak value increases from 0.0154 to 0.02117 with an increment increases to 0.00577, which is 4.15 times of the original increment. The right peak value increases from 0.00739 to 0.013 with an increment of 0.00561, which is 13.68 times the original increment. In addition, ϵ increases first and then decreases with the increase of H. When $H = -20$, i is 1.79, and when $H = -8$, i reaches the maximum of 2.48. When $H = 0$, i decreases to 1.63.

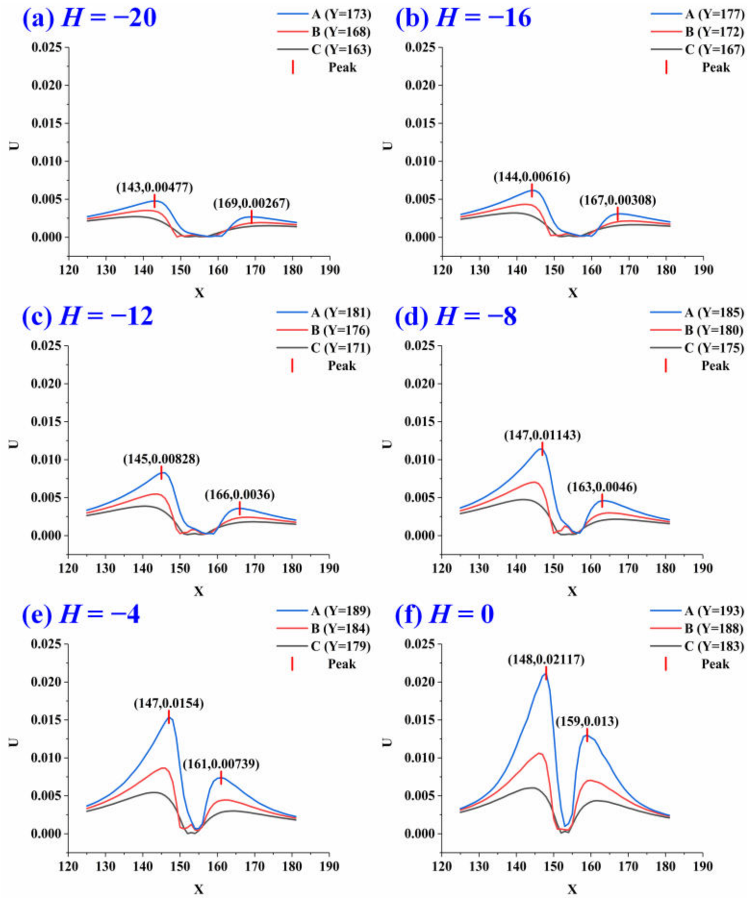

Fig. 13. Velocity distribution on three groups of horizontal lines (A, B and C) under different vertical deviations: (a) $H = -20$, (b) $H = -16$, (c) $H = -12$, (d) $H = -8$, (e) $H = -4$, (f) $H = 0$

3.2.3. Temporal evolution of tea span and leaf tip x coordinates under different vertical deviations

The quantitative analysis of the deformation characteristics of tea shoot in each time period is of great importance to clarify the mechanism of negative pressure guidance. Fig. 14 shows the time evolution of tea span and leaf tip x coordinates under six different vertical deviations. Comparison reveals that the development trend of each polyline in Fig. 14 is similar to that in Fig. 9. Figs. 14(f) and 9(d) correspond to the same simulation test. The polyline trend displays that after 100,000 steps, the flow field corresponding to Figs. 14(e) and 14(f) has reached a stable state, whereas the flow field corresponding to Figs. 14(a)–14(d) is not stable yet, so the stable value needs to be obtained through linear fitting. In addition, the law can be determined: As H increases, d_f becomes smaller, and the deformation speed is faster.

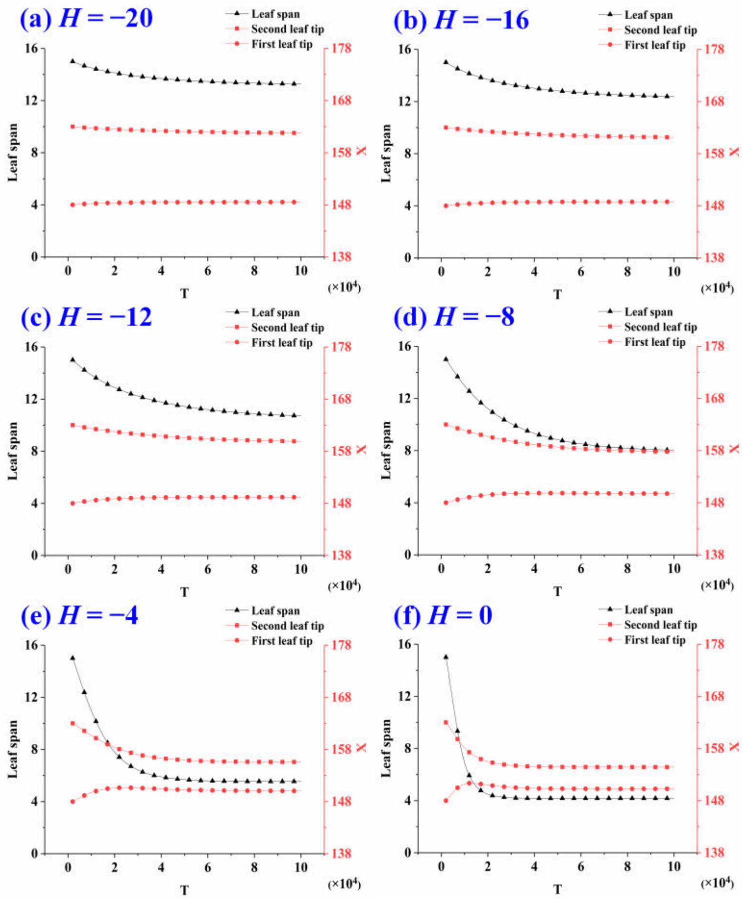

Fig. 14. Temporal evolution of tea span and leaf tip x coordinates under different vertical deviations: (a) $H = -20$, (b) $H = -16$, (c) $H = -12$, (d) $H = -8$, (e) $H = -4$, (f) $H = 0$

Fig. 15 demonstrates the polyline of d_s changing with H. The decrement of d_s first increases and then decreases with the increase of H. When H increases from −20 to −16, the decrement of d_s is 0.95. When H increases from −12 to −8, the decrement of d_s increases to 2.57. However, when H increases from −4 to 0, the decrement of d_s decreases to 1.37. The main reason is that when θ_2 is large, the airflow velocity has a great influence on d, and the increment of the fluid velocity around the tea increases with the increase of H. Therefore, at the beginning, the decrement of d_s is positively correlated with H. When $H \geq -8$, θ_2 is small enough to reduce the increment of torque provided by fluid. Therefore, when H continues to increase, the decrement of d_s begins to decrease.

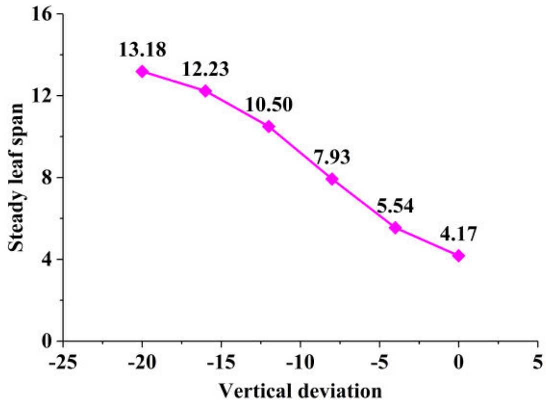

Fig. 15. Steady leaf span changing with vertical deviation

Fig. 16 is a polyline graph of T changing with P. Fig. 16 shows that with the increase of H, T first increases and then decreases. The data show that T is 22,655 at $H = –20$, increases to 24,197 at $H = −16$ and decreases to 3,068 at $H = 0$, which means that when $H = 0$, the deformation efficiency of tea shoot is the highest.

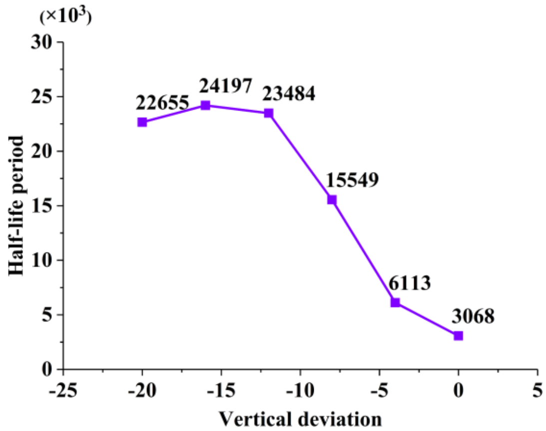

Fig. 16. Half-life period changing with vertical deviation

3.3. Effect of horizontal deviation W on deformation of tea shoot

3.3.1. Time evolution of velocity, vorticity and tea shoot under different horizontal deviations

Fig. 17(a) illustrates the time evolution of velocity, vorticity and tea shoot at $W = −8$. Fig. 17(a1) displays that tea is located on the left under pipe mouth. Two flow channels with similar sizes are in the initial period. A positive vortex is formed at Q_1 and the left side of Q_2, and a negative vortex is formed at the right side of Q_2. In the process of negative pressure guidance, the left flow channel gradually shrinks, and the right flow channel gradually expands. Fig. 17(a2) shows that the positive vortices at Q_1 and the left side of Q_2 are connected. Fig. 17(a3) illustrates that SL continues to rotate counter clockwise, and the vorticity of the positive vortex at the left side of Q_2 increases. Finally, Fig. 17(a4) displays that the right flow channel is remarkably larger than the left flow channel, and the negative vortex at the right side of Q_2 is connected to the negative vortex at the left side of the pipe mouth.

Fig. 17(b) describes the time evolution of velocity, vorticity and tea shoot at $W = 8$. Fig. 17(b1) describes that tea is located on the right under pipe mouth. Two flow channels are in the initial period, and the left channel is considerably larger than the right flow channel. Furthermore, a negative vortex is formed at the right side of Q_1 and Q_2, and a positive vortex is formed at the left side of Q_1. In the process of negative pressure guidance, the left flow channel first increases and then decreases, and the right flow channel first decreases and then increases. Fig. 17(b2) shows that the positive vortex at the left side of Q_1 extends and connects to the positive vortex at the right side of the pipe mouth, and the size of the negative vortex at Q_2 decreases. When SL rotates to the position shown in Fig. 17(b3), the right flow channel disappears, and until SL continues to rotate to the position shown in Fig. 17(b4), the right channel reappears. At this time, SL has rotated to the left of the tea centre.

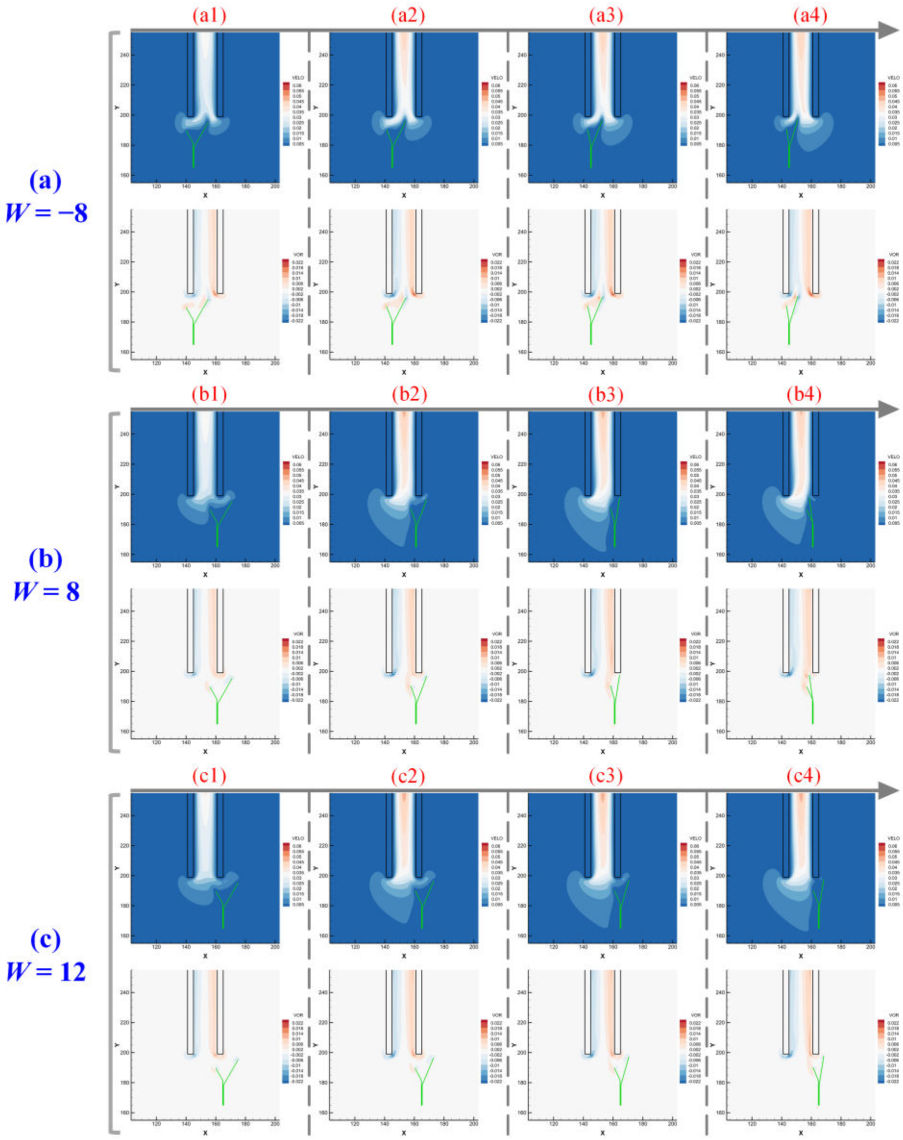

Fig. 17. Time evolution of velocity, vorticity and tea shoot under different horizontal deviations: (a) $W = -8$, (b) $W = 8$, (c) $W = 12$

Fig. 17(c) describes the time evolution of velocity, vorticity and tea shoot at $W = 12$. In Fig. 17(c1), two flow channels are in the initial period, and the left flow channel is remarkably larger than the right flow channel. Moreover, a positive vortex and a negative vortex are formed on the left and right sides of Q_1, respectively, and a negative vortex is formed at Q_2. Over time, the left flow channel gradually increases, and the right flow channel gradually decreases. Figs. 17(c2)–17(c4) show the positive vortex at the left side of Q_1 expands gradually, the negative vortex at Q_2 expands first and then shrinks, and the negative vortex at the right side of Q_1 gradually shrinks. In the final state, the right flow channel almost disappears. In addition, the positive vortex at the left side of Q_1 connects to the positive vortex at the right side of pipe mouth.

Finally, based on the above discussion, with the increase of W, d_f first decreases and then increases.

3.3.2. Velocity distribution under different horizontal deviations

By analysing the velocity distribution of the fluid around the tea shoot, the fluid–tea coupling characteristics can be studied better. Fig. 18 illustrates the final velocity of fluid points on three groups of horizontal lines (A, B and C) under six different horizontal deviations, and Fig. 5 shows the horizontal lines (A, B and C).

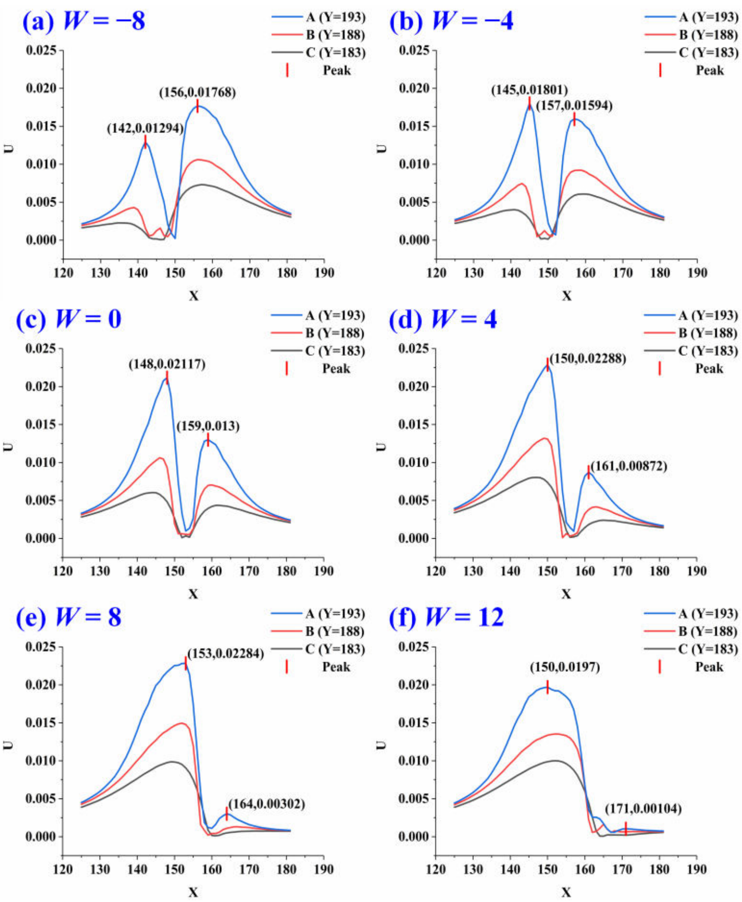

Fig. 18. Velocity distribution on three groups of horizontal lines (A, B and C) under different horizontal deviations: (a) $W = -8$, (b) $W = -4$, (c) $W = 0$, (d) $W = 4$, (e) $W = 8$, (f) $W = 12$

Waveform comparison reveals that the polyline in Fig. 18 has two mountains and one valley. Taking the velocity polyline corresponding to A as an example, with the increase of W, the left peak value and the x coordinate of the left peak first increases and then decreases, the right peak value gradually decreases, and the x coordinate of right peak gradually increases. Moreover, the valley gradually shifts to the right because when W increases, the whole tea shoot shifts to the right, and the area blocked by tea shoot on the horizontal line also shifts to the right. In summary, W has no remarkable effect on the average velocity of the fluid point but influences the magnitude and location of the velocity peak value.

Data analysis finds that the decrement of the right peak value increases first and then decreases with the increase of W. When W increases from −8 to −4, the right peak value decreases from 0.01768 to 0.01594, and the decrement is 0.00172. When W increases from 4 to 8, the right peak value decreases from 0.00872 to 0.00302, and the decrement increases to 0.0057. However, when W increases from 8 to 12, the right peak value decreases from 0.00302 to 0.00104, and the decrement decreases to 0.00198. In addition, W is positively correlated to i. When $W = -8$, i is 0.73, and when $W = 12$, i increases to 18.94.

3.3.3. Temporal evolution of tea span and leaf tip x coordinates under different horizontal deviations

Fig. 19 describes the time evolution of tea span and leaf tip x coordinates under six different horizontal deviations. As W increases, the whole tea moves to the right, so the initial X_1 and X_2 gradually increase. Moreover, the polyline trend reveals that after 100,000 steps, the flow field corresponding to Figs. 19(a)–19(d) has reached a stable state, whereas the flow field corresponding to Figs. 19(e) and 19(f) is not stable yet, and a linear fitting method is required to obtain stable values. In addition, with the increase of W, d_f decreases first and then increases, the final rotation angle of SL first increases and then decreases, and the final rotation angle of FL becomes smaller.

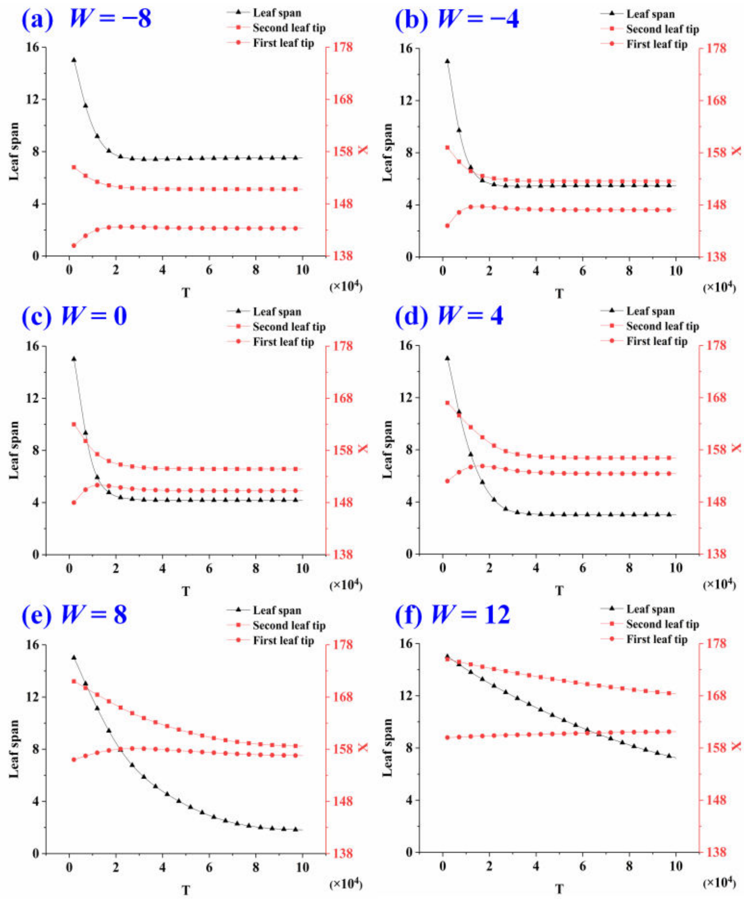

Fig. 19. Temporal evolution of tea span and leaf tip x coordinates under different horizontal deviations:(a) $W = -8$, (b) $W = -4$, (c) $W = 0$, (d) $W = 4$, (e) $W = 8$, (f) $W = 12$

To make the change of d_s more intuitive, Fig. 20 is plotted to show the polyline of d_s changing with W. When $W \leq 8$, d_s decreases with the increase of W, and the decrement is similar. However, when W increases from 8 to 12, d_s increases from 1.78 to 4.48. The main reason is that when $W \leq 8$, SL is not far enough from the pipe mouth, and the velocity of the surrounding fluid point is large, so that it can still rotate greatly. When $W = 12$, SL is far enough from the pipe mouth, resulting in a decrease in the rotation of SL.

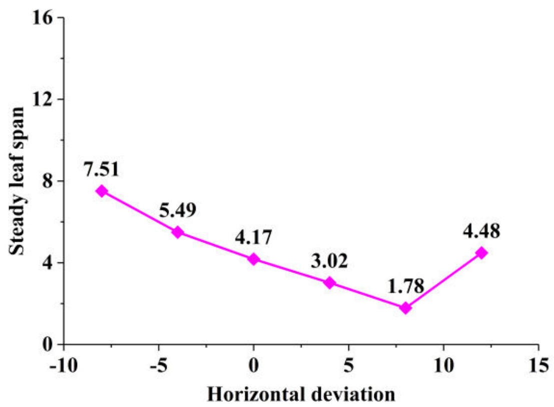

Fig. 20. Steady leaf span changing with horizontal deviation

To make the deformation efficiency of tea shoot more intuitive, Fig. 21 is drawn to show the polyline of T changing with W. With the increase of horizontal deviation W, T decreases first and then increases, which means the deformation efficiency of tea shoot increases first and then decreases. Based on the data, T is 9,413 at $W = -8$, decreases to 3,068 at $W = 0$ and increases to 45,489 at $W = 12$, which is much larger than 7,079 steps at $W = 8$.

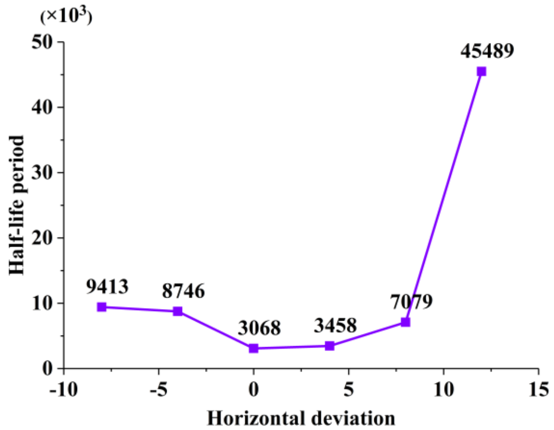

Fig. 21. Half-life period changing with horizontal deviation

3.4. Effect of position deviation (H and W) on deformation of tea shoot

Fig. 22 shows d_s variation under different position deviations (H and W) by isoline map. The isoline is concave. Therefore, when W is constant, the greater H is, the smaller d_s is. When H is constant, d_s decreases first and then increases with the increase of W. Furthermore, when d_s is the minimum, the whole tea is located below the right side of the pipe mouth, that is, the side where SL is located. The reason is that SL is longer and is greatly affected by the fluid. In addition, the lowest point of each isoline is defined as the minimum point, and the point–line diagram is drawn. With the increase of d_s, the vertical deviation H at the minimum point gradually decreases, whereas the horizontal deviation W at the minimum first decreases, then increases and finally decreases. When d_s is 2, the W at the minimum point is 7.66. When d_s increases to 3, the W at the minimum point decreases to 6.39. When d_s increases to 4, the W at the minimum point increases to 6.61. Finally, as d_s continues to increase, the W at the minimum point gradually decreases to 0.77.

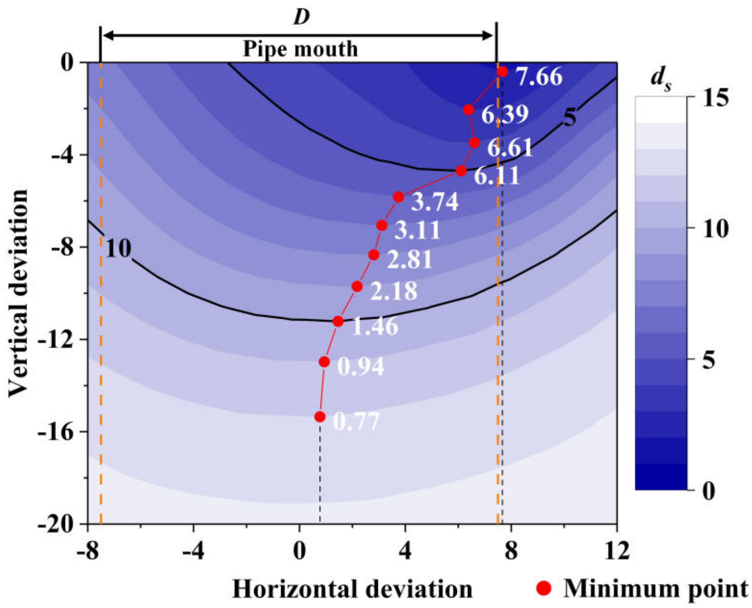

Fig. 22 Effect of position deviation (H and W) on steady leaf span

Fig. 23 illustrates variation law of T obtained by statistical 36 groups of simulation test results. The distribution of T is asymmetrical because tea itself is asymmetrical. Fig. 23 is divided into five areas (R_1, R_2, R_3, R_4, R_5) from large to small according to T. The T of area R_1 is short, all within 10,000 steps because area R_1 is near the pipe mouth, the velocity of the surrounding fluid point is large and the deformation efficiency of tea shoot is high. Two main reasons explain the gradual lengthening of T in areas R_2 and R_3. Firstly, some locations are far from the pipe mouth, where the velocity of the fluid around the tea is low, and the deformation speed is slow. Secondly, some locations are close to the pipe mouth, where the deformation of tea shoot is large, thus lengthening T. In addition, areas R_4 and R_5 are located at the right side of the pipe mouth. The main reason for the gradual lengthening of T is the decrease of fluid velocity.

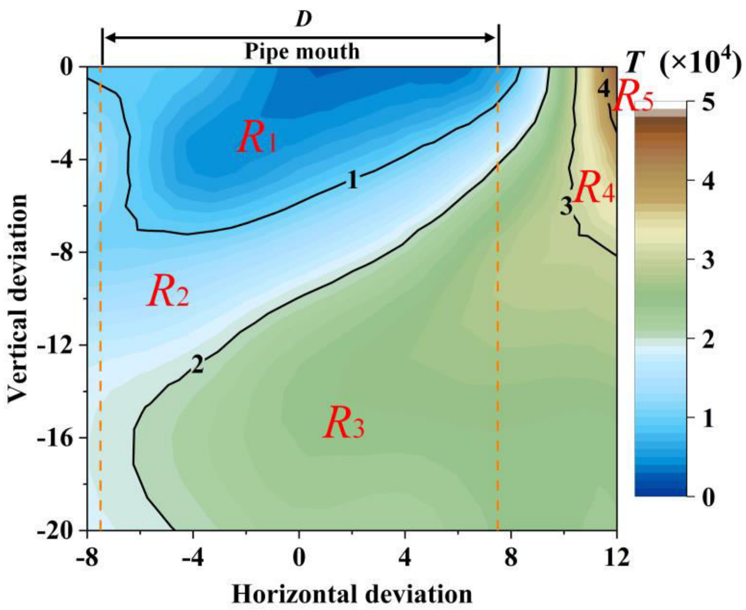

Fig. 23. Effect of position deviation (H and W) on half-life period

4. Conclusions

In this paper, a new 'Y-type' tea shoot model is established according to the physical properties of tea shoot, which can be used to study the deformation of single tea shoot. Moreover, the deformation law of tea shoot under negative pressure guidance is studied by using IB-LBM. The effectiveness of the tea shoot model is verified by simulation test, and the effect of pressure and position deviation on the deformation of tea shoot is quantitatively analysed. The conclusions are as follows:

Firstly, pressure P determines the velocity of the fluid in the flow field. When the tea centre is fixed at the reference point and P decreases, the velocity of the fluid in the flow field increases, leading to the decrease of d_s. In addition, the polylines of d_s and T changing with P are analysed, and the results show that T and the decrement of d_s also decrease with the decrease of P. When $P = 0.984$, d_s and T achieve minimum values of 3.81 and 2,177, respectively.

Secondly, when P is fixed, with the increase of the vertical deviation H, the d_s decreases, and T increases first and then decreases. When $H = 0$, d_s and T achieve minimum values of 4.17 and 3,068, respectively. Moreover, with the increase of the horizontal deviation W, d_s and T decrease first and then increase. When $W = 8$, d_s achieves a minimum value of 1.78, and T achieves a minimum value of 3,068 at $W = 0$.

Finally, the combined effect of H and W is considered. When P is fixed, with the decrease of H, W needs to decrease first, then increase and finally decrease again to minimize d_s. In addition, the area with small T are concentrated near the pipe mouth and shows an asymmetric distribution.

The effects of pressure P, vertical deviation H and horizontal deviation W on the deformation of tea shoot have been preliminarily revealed. Leaf bending deformation and negative pressure dynamic guidance will be further studied. The current study results show that the 'Y-type' tea shoot model can better reflect the deformation characteristics of a single tea shoot, and a numerical calculation method is expected to be developed further to optimize the picking end effector of famous tea.

5. CRediT authorship contribution statement

Yingpeng Zhu: Conceptualization, Methodology, Data analysis, Writing – original draft. Yikun Wei: Conceptualization, Writing – review, Funding acquisition. Zhengdao Wang: Conceptualization, Methodology, Data analysis. Rongyang Wang: Conceptualization, Methodology, Funding acquisition. Chuanyu Wu: Project administration, Funding acquisition. Jianneng Chen: Project administration, Conceptualization. Junhua Tong: Writing – review, Supervision.

6. Declaration of competing interest

The authors declare that they have no known competing financial interests or personal relationships that could have appeared to influence the work reported in this paper.

7. Acknowledgements

The authors gratefully acknowledge the financial support provided by the China Agriculture Research System of MOF and MARA, the National Natural Science Foundation of China (Nos. 51975537 and 52105283), and the Natural Science Foundation Key Projects of Zhejiang Province (LZ22E060002). Any opinions, findings, conclusions, or recommendations expressed in this publication are those of the authors and do not necessarily reflect the view of Zhejiang Sci-Tech University.

8. References

Wang, X., Han, C., Wu, W., Xu, J., Zhang, Q., Chen, M., Hu, Z., Zheng, Z., 2021. Fundamental understanding of tea growth and modeling of precise tea shoot picking based on 3-D coordinate instrument. Processes 9(6), 1059. https://doi.org/10.3390/pr9061059

Han, Y., Xiao, R., Song, Y., Ding, Q., 2019. Design and evaluation of tea-plucking machine for improving quality of tea. Appl. Eng. Agric. 35(6), 979–986. https://doi.org/10.13031/aea.13116

Li, Y., He, L., Jia, J., Lv, J., Chen, J., Qiao, X., Wu, C., 2021. In-field tea shoot detection and 3D localization using an RGB-D camera. Comput. Electron. Agr. 185, 106149. https://doi.org/10.1016/j.compag.2021.106149

Tian, J., Zhu, H., Liang, W., Chen, J., Wen, F., Long, Z., 2021. Research on the application of machine vision in tea autonomous picking. Journal of Physics: Conference Series 1952(2), 022063. https://doi.org/10.1088/1742-6596/1952/2/022063

Qin, G., Zhao, Y., Xiao, H., Jin, Y., Xu, L., Chen, Y., 2014. 4CZ-12 intelligent tea harvest robot design and field experiment. Journal of Chinese Agricultural Mechanization 35(1), 152-156, 169. https://doi.org/10.3969/j.issn.2095-5553.2014.01.035

Hao, M., Chen, Y., Pan, Z., Sun, Y., 2018. Development of bionic plucking finger for high-quality green tea. Food & Machinery 34(10), 86-90. https://doi.org/10.13652/j.issn.1003-5788.2018.10.018

Motokura, K., Takahashi, M., Ewerton, M., Peters, J., 2020. Plucking motions for tea harvesting robots using probabilistic movement primitives. IEEE Robot. Autom. Lett. 5(2), 3275–3282. https://doi.org/10.1109/lra.2020.2976314

Zhu, Y., Wu, C., Tong, J., Chen, J., He, L., Wang, R., Jia, J., 2021. Deviation tolerance performance evaluation and experiment of picking end effector for famous tea. Agriculture 11(2), 128. https://doi.org/10.3390/agriculture11020128

Han, D., Zhang, D., Jing, H., Yang, L., Cui, T., Ding, Y., Wang, Z., Wang, Y., Zhang, T., 2018. DEM-CFD coupling simulation and optimization of an inside-filling air-blowing maize precision seed-metering device. Comput. Electron. Agr. 150, 426–438. https://doi.org/10.1016/j.compag.2018.05.006

Zheng, W., Jiang, Y., Ma, X., Qi, L., 2019. Development of a liquid-jet nozzle for fertilizer injection in paddy fields using CFD. Comput. Electron. Agr. 167, 105061. https://doi.org/10.1016/j.compag.2019.105061

Ma, L., Wei, L., Pei, X., Zhu, X., Xu, D., 2019. CFD-DEM simulations of particle separation characteristic in centrifugal compounding force field. Powder Technol. 343, 11–18. https://doi.org/10.1016/j.powtec.2018.11.016

Kuang, S., Zhou, M., Yu, A., 2020. CFD-DEM modelling and simulation of pneumatic conveying: A review. Powder Technol. 365, 186–207. https://doi.org/10.1016/j.powtec.2019.02.011

Zhu, H., Li, H., Zhang, C., Li, J., Zhang, H., 2019. Performance characterization of the UAV chemical application based on CFD simulation. Agronomy 9(6), 308. https://doi.org/10.3390/agronomy9060308

Guzman, L., Chen, Y., Landry, H., 2020. Coupled CFD-DEM simulation of seed flow in an air seeder distributor tube. Processes 8(12), 1597. https://doi.org/10.3390/pr8121597

Xiong, Q., Madadi-Kandjani, E., Lorenzini, G., 2014. A LBM–DEM solver for fast discrete particle simulation of particle–fluid flows. Continuum Mech. Therm. 26(6), 907–917. https://doi.org/10.1007/s00161-014-0351-z

Tao, S., He, Q., Chen, B., Yang, X., Huang, S., 2018. A direct force model for Galilean invariant lattice Boltzmann simulation of fluid-particle flows. Int. J. Mod. Phys. C 29(03), 1850021. https://doi.org/10.1142/s0129183118500213

Wang, Z., Wei, Y. K., Qian, Y., 2018. Study of flapping filaments using the immersed boundary-lattice Boltzmann method. Text. Res. J. 89(15), 3127–3136. https://doi.org/10.1177/0040517518807455

Wang, L., Tian, F., 2019a. Numerical simulation of flow over a parallel cantilevered flag in the vicinity of a rigid wall. Phys. Rev. E 99(5), 053111. https://doi.org/10.1103/physreve.99.053111

Tang, C., Lu, X., 2016. Self-propulsion of a three-dimensional flapping flexible plate. J. Hydrodyn. Ser. B 28(1), 1–9. https://doi.org/10.1016/s1001-6058(16)60602-9

Wang, R., Wei, Y., Wu, C., Sun, L., Zheng, W., 2019b. Numerical simulation of motion characteristics of flexible fresh tea leaf in Poiseuille shear flow via combined immersed boundary–lattice Boltzmann method. Int. J. Mod. Phys. C 30(05), 1950038. https://doi.org/10.1142/s0129183119500384

Wu, J., Shu, C., 2010. Particulate flow simulation via a boundary condition-enforced immersed boundary-lattice Boltzmann scheme. Commun. Comput. Phys.7 (4), 793–812. https://doi.org/10.4208/cicp.2009.09.054

Qian, Y., D'Humières, D., Lallemand, P., 1992. Lattice BGK models for Navier-Stokes equation. Europhys. Lett. 17(6), 479–484. https://doi.org/10.1209/0295-5075/17/6/001

Guo, Z., Zheng, C., Shi, B., 2002. Discrete lattice effects on the forcing term in the lattice Boltzmann method. Phys. Rev. E 65(4), 046308. https://doi.org/10.1103/physreve.65.046308

Wang, R., He, Y., Chen, L., Zhu, Y., Wei, Y, 2022. Numerical simulations of flow around three cylinders using momentum exchange-based immersed boundary-lattice Boltzmann method. Ocean Engineering 247, 110706. https://doi.org/10.1016/j.oceaneng.2022.110706

(33) WhatsApp × | Review for Biosystems Engineerin × | +

mail.google.com/mail/u/0/?tab=rm#inbox/FMfcgzGpFqVHSRXzGpRVtSShJrKbRpdH

Gmail | YouTube | Maps | WhatsApp | Kuliah Online Unive... | New Tab

Gmail

Search mail

Compose

Inbox 153
Starred
Snoozed
Important
Sent

Meet
New meeting
Join a meeting

Hangouts
Eflita
No recent chats
Start a new one

1 of 1,944

Review for Biosystems Engineering - next steps

Inbox ×

Fernando Auat Cheein <em@editorialmanager.com>
to me

2:00 PM (3 hours ago)

May
31
Tue

Review Due

When Tue May 31, 2022 (WIB)
Who Biosystems Engineering*
Add to calendar »

Agenda

Tue May 31, 2022

No earlier events

All day Review Due

No later events

This is an automated message.

Manuscript Number: YBENG-D-22-00513

Numerical simulation for deformation characteristic of tea shoot under negative pressure guidance by the immersed boundary–lattice Boltzmann method

Yingpeng Zhu; Yikun Wei; Zhengdao Wang; Rongyang Wang; Chuanyu Wu; Jianneng Chen; Junhua Tong

Dear Dr. Yohana,

24°C Berawan 17.17 10/05/2022

Dear Dr. Yohana,

Thank you for agreeing to review the above referenced manuscript.

Timely reviews are of utmost importance to authors, therefore I would be grateful if you would please submit your review by May 31, 2022.

Please read the following instructions carefully before starting your evaluation:

https://www.elsevier.com/reviewers/how-to-conduct-a-review

Please also note these important ethical guidelines all reviewers are asked to follow:

* You should treat the manuscript and your review as confidential. You must not share your review or information about the review process with anyone without the agreement of the editors and authors involved, even after publication. This also applies to other reviewers' "comments to author" which are shared with you on decision (and vice versa).

* If you suspect plagiarism, fraud or have other ethical concerns, please raise your suspicions with the editor, providing as much detail as possible.

* Any suggestion you make that the author include citations to your (or your associates') work must be for genuine scientific reasons and not with the intention of increasing your citation counts or enhancing the visibility of your work (or those of your associates).

When you are ready to submit your review, you may access the submission record here https://www.editorialmanager.com/ybeng/l.asp?i=191788&l=K3ECAMMT. Please click on the "Submit Recommendation" link to enter your comments.

(34) WhatsApp | Review for Biosystems Engineerin

mail.google.com/mail/u/0/?tab=rm#inbox/FMfcgzGpFqVHSRXzGpRVtSShJrKbRpdH

Gmail YouTube Maps WhatsApp Kuliah Online Unive... New Tab

Gmail

Search mail

Compose

Inbox 153

Starred

Snoozed

Important

Sent

Meet

New meeting

Join a meeting

Hangouts

Eflita

No recent chats

Start a new one

1 of 1,944

If, for any reason, the above link does not work, please log in as a reviewer at https://www.editorialmanager.com/ybeng/.

As a reviewer you are entitled to complimentary access to ScienceDirect and Scopus. This 30-day access can be activated in the [Rewards] section of your profile in Reviewer Hub (reviewerhub.elsevier.com) and you have six months to activate it.

Please visit the Elsevier Reviewer Hub (reviewerhub.elsevier.com) to manage all your refereeing activities for this and other Elsevier journals on Editorial Manager.

I look forward to receiving your review soon.

Thank you in advance for your contribution and time.

Kind Regards,

Fernando Auat Cheein
Associate Editor
Biosystems Engineering

More information and support
FAQ: How can I submit my review in Editorial Manager?

https://service.elsevier.com/app/answers/detail/a_id/28465/supporthub/publishing/

24°C Berawan 17.18 10/05/2022

(34) WhatsApp | Review for Biosystems Engineerin

mail.google.com/mail/u/0/?tab=rm#inbox/FMfcgzGpFqVHSRXzGpRVtSShJrKbRpdH

Gmail YouTube Maps WhatsApp Kuliah Online Unive... New Tab

Gmail

Search mail

Compose

Inbox 153
Starred
Snoozed
Important
Sent

Meet
New meeting
Join a meeting

Hangouts
Eflita
No recent chats
Start a new one

FAQ: How can I submit my review in Editorial Manager?

https://service.elsevier.com/app/answers/detail/a_id/28465/supporthub/publishing/

You will find guidance and support on reviewing, as well as information including details of how Elsevier recognizes reviewers, on Elsevier's Reviewer Hub:
https://www.elsevier.com/reviewers
FAQ: How can I reset a forgotten password?
https://service.elsevier.com/app/answers/detail/a_id/28452/supporthub/publishing/
For further assistance, please visit our customer service site: https://service.elsevier.com/app/home/supporthub/publishing/
Here you can search for solutions on a range of topics, find answers to frequently asked questions, and learn more about Editorial Manager via interactive tutorials. You can also talk 24/7 to our customer support team by phone and 24/7 by live chat and email

---

In compliance with data protection regulations, you may request that we remove your personal registration details at any time. (Use the following URL: https://www.editorialmanager.com/ybeng/login.asp?a=r). Please contact the publication office if you have any questions.

Review_Due.ics Download

Reply Forward

24°C Berawan 17.18 10/05/2022

Biosystems Engineering

Numerical simulation for deformation characteristic of tea shoot under negative pressure guidance by the immersed boundary–lattice Boltzmann method

1. Apart from what is mentioned in subsection 2.2, are there no other properties of tea leaves that is included in the simulation software? i.e. leaf weight, etc.
2. in Figure 3, 20D is there a separate standard, or is there a certain reason for using the existing size?
3. Do the numbers in Figure 4 have certain units? Perhaps P and others
4. Can you mention anything that proves that your numerical calculations are in accordance with the simulation test? and if so, what error value did you obtain?
5. To make it easier for readers, the Legend in Figures 6, 12, 17, should be enlarged, and the image quality should be improved.
6. In Figures 6, 12, and 17 there are two contour views (Top and Bottom), what does each of these contours show?
7. In your opinion, what might happen if the position of the pipe mouth is not parallel to the position of the leaf? (in this case, if there is a certain angle)
8. In Line 26, you mention one of the abstract keywords of the IB-LBM, while there is no explanation of the IB-LBM in the Abstract itself.
9. Did you make up your own terms for “Y-type” Tea Shoot model, or are there several other types? If there are any, mention them and give a brief explanation.
10. In Row 120 you mentioned the angle of the first and second leaf to be 30^{o}, where did you obtain that value?
11. What type of CFD simulation are you using, Steady or Transient? and explain the purpose of using it?

Biosystems ENGINEERING
Editorial Manager

Role: Reviewer Username: EflitaYohana

Review Thank You

Thank you for reviewing Manuscript Number YBENG-D-22-00513.

Return to Main Menu

Log out of Editorial Manager

mail.google.com/mail/u/0/?tab=rm#inbox/FMfcgzGpFqdDfXNpckZscBpdckKfLXGX

Gmail YouTube Maps WhatsApp Kuliah Online Unive... New Tab

Gmail

Search mail

Compose

Inbox 158

Starred

Snoozed

Important

Sent

Meet

New meeting

Join a meeting

Hangouts

Eflita

No recent chats

Start a new one

1 of 1,959

Thank you for reviewing for Biosystems Engineering

Inbox

Biosystems Engineering <em@editorialmanager.com> 7:17 PM (1 minute ago)

to me

Manuscript Number: YBENG-D-22-00513

Numerical simulation for deformation characteristic of tea shoot under negative pressure guidance by the immersed boundary–lattice Boltzmann method

Yingpeng Zhu; Yikun Wei; Zhengdao Wang; Rongyang Wang; Chuanyu Wu; Jianneng Chen; Junhua Tong

Dear Dr. Yohana,

Thank you for reviewing the above referenced manuscript. I greatly appreciate your contribution and time, which not only assisted me in reaching my decision, but also enables the author(s) to disseminate their work at the highest possible quality. Without the dedication of reviewers like you, it would be impossible to manage an efficient peer review process and maintain the high standards necessary for a successful journal.

I hope that you will consider Biosystems Engineering as a potential journal for your own submissions in the future.

As a token of appreciation, we would like to provide you with a review recognition certificate on Elsevier Reviewer Hub (reviewerhub.elsevier.com). Through the Elsevier Reviewer Hub, you can also keep track of all your reviewing activities for this and other Elsevier journals on Editorial Manager.

If you have not yet activated your 30 day complimentary access to ScienceDirect and Scopus, you can still do so via the [Rewards] section of your profile in

26°C 19.19 16/05/2022

(26) | Than | Edito | Edito | Num | Edito | Revie | What | Edito | Edito | goog

mail.google.com/mail/u/0/?tab=rm#inbox/FMfcgzGpFqdDfXNpckZscBpdckKfLXGX

Gmail | YouTube | Maps | WhatsApp | Kuliah Online Unive... | New Tab

Gmail

Search mail

Compose

Inbox 158

Starred

Snoozed

Important

Sent

Meet

New meeting

Join a meeting

Hangouts

Eflita

No recent chats

Start a new one

1 of 1,959

If you have not yet activated your 30 day complimentary access to ScienceDirect and Scopus, you can still do so via the [Rewards] section of your profile in Reviewer Hub (reviewerhub.elsevier.com).
You can always claim your 30-day access period later, however, please be aware that the access link will expire six months after you have accepted to review.

Kind regards,

Fernando Auat Cheein
Associate Editor
Biosystems Engineering

More information and support

You will find guidance and support on reviewing, as well as information including details of how Elsevier recognizes reviewers, on Elsevier's Reviewer Hub: https://www.elsevier.com/reviewers

FAQ: How can I reset a forgotten password?
https://service.elsevier.com/app/answers/detail/a_id/28452/supporthub/publishing/
For further assistance, please visit our customer service site: https://service.elsevier.com/app/home/supporthub/publishing/
Here you can search for solutions on a range of topics, find answers to frequently asked questions, and learn more about Editorial Manager via interactive tutorials. You can also talk 24/7 to our customer support team by phone and 24/7 by live chat and email

26°C 19.19 16/05/2022